

**PHOTON 2017**

**CERN**

**May 26th, 2017**

# **Isolated photon, photon+jet and diphoton results in ATLAS**

**J. Terrón (Universidad Autónoma de Madrid)**

**On behalf of the ATLAS Collaboration**

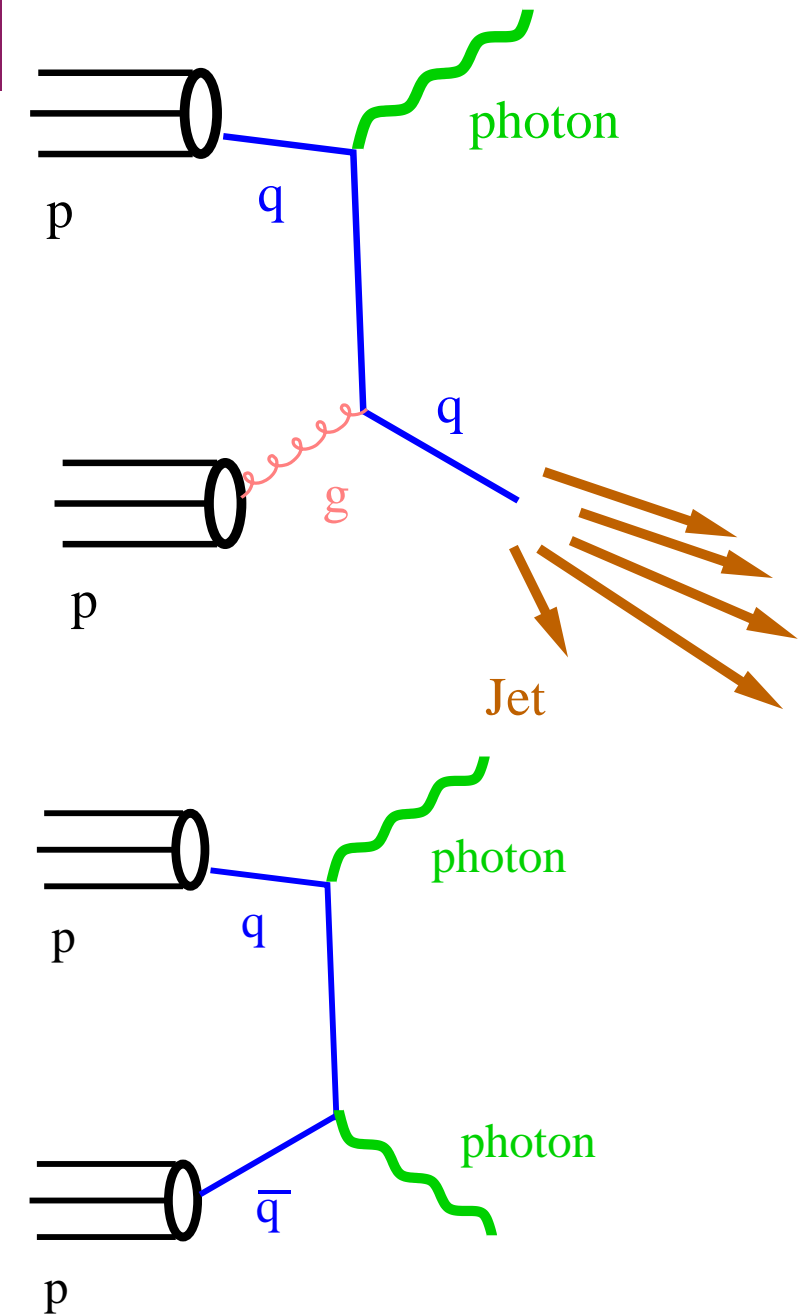
## ● **Outline**

- Physics with photons
- Inclusive photon production at 13 TeV
- Photon + jet(s) production at 8 TeV
- Photon pair production at 8 TeV
- Summary



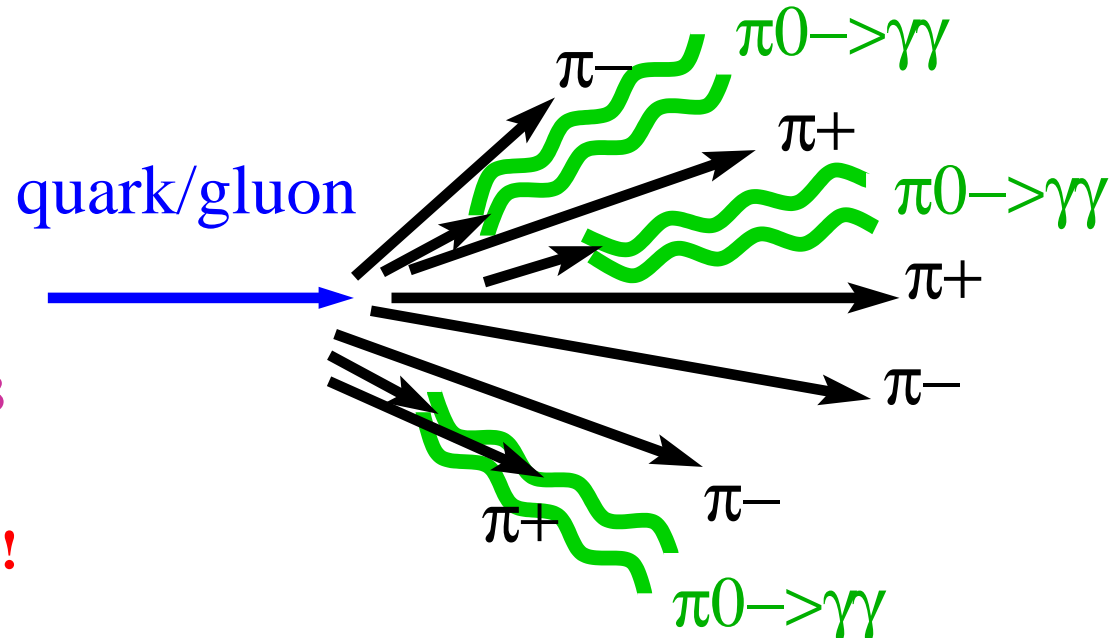
## Photon production in $pp$ collisions at LHC

- Photon production in  $pp$  collisions
  - allows tests of perturbative QCD predictions
  - provides information on the proton PDFs
- Possibilities to study inclusive production of photons or in association with jets
- Prompt photons represent a cleaner probe of the hard interaction than jet production
- Prompt-photon measurements aid searches involving photons or  $E_T^{\text{miss}} + \text{jets}$  (through ratios  $Z + \text{jets}/\gamma + \text{jets}$ )
- Diphoton production is of special interest as the major background to  $H \rightarrow \gamma\gamma$

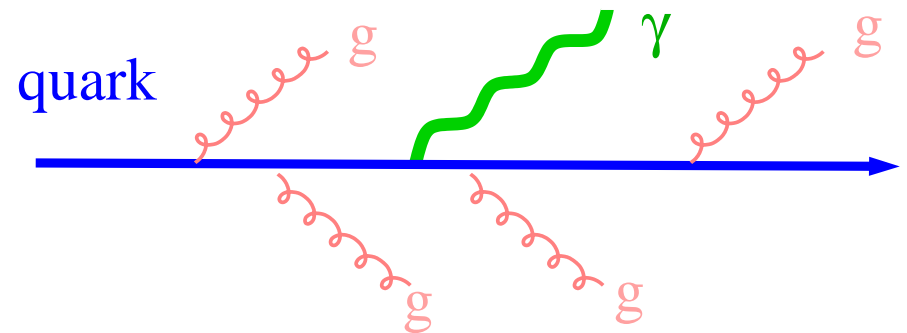


## Other sources of photons

- Quarks and gluons are sources of photons
  - Quarks and gluons fragment mostly into pions and, by isospin symmetry, 1/3 are  $\pi^0$ 's, which decay into two photons
  - ⇒  $\gamma$ 's are produced copiously inside jets!

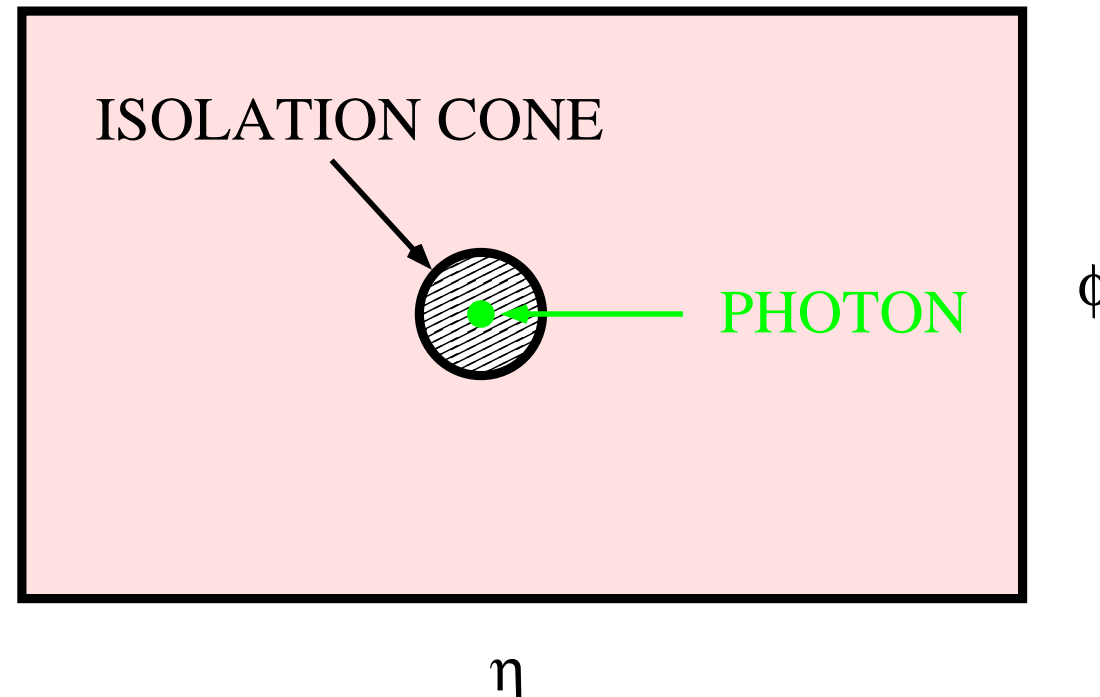
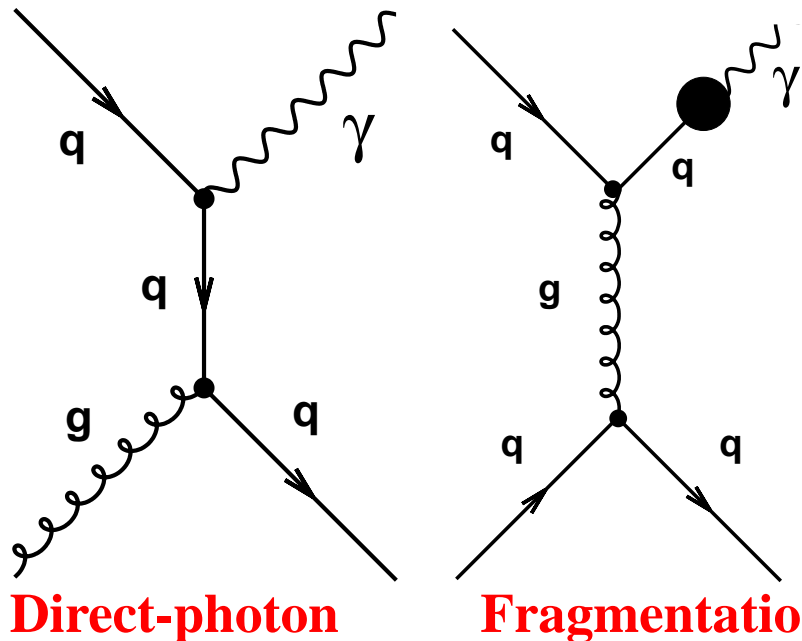


- Quarks have electric charge and radiate photons
  - ⇒ fragmentation function  $D_{q/g}^\gamma(z, \mu_f)$



⇒ Distinct feature: these photons are inside jets, i.e. not isolated!

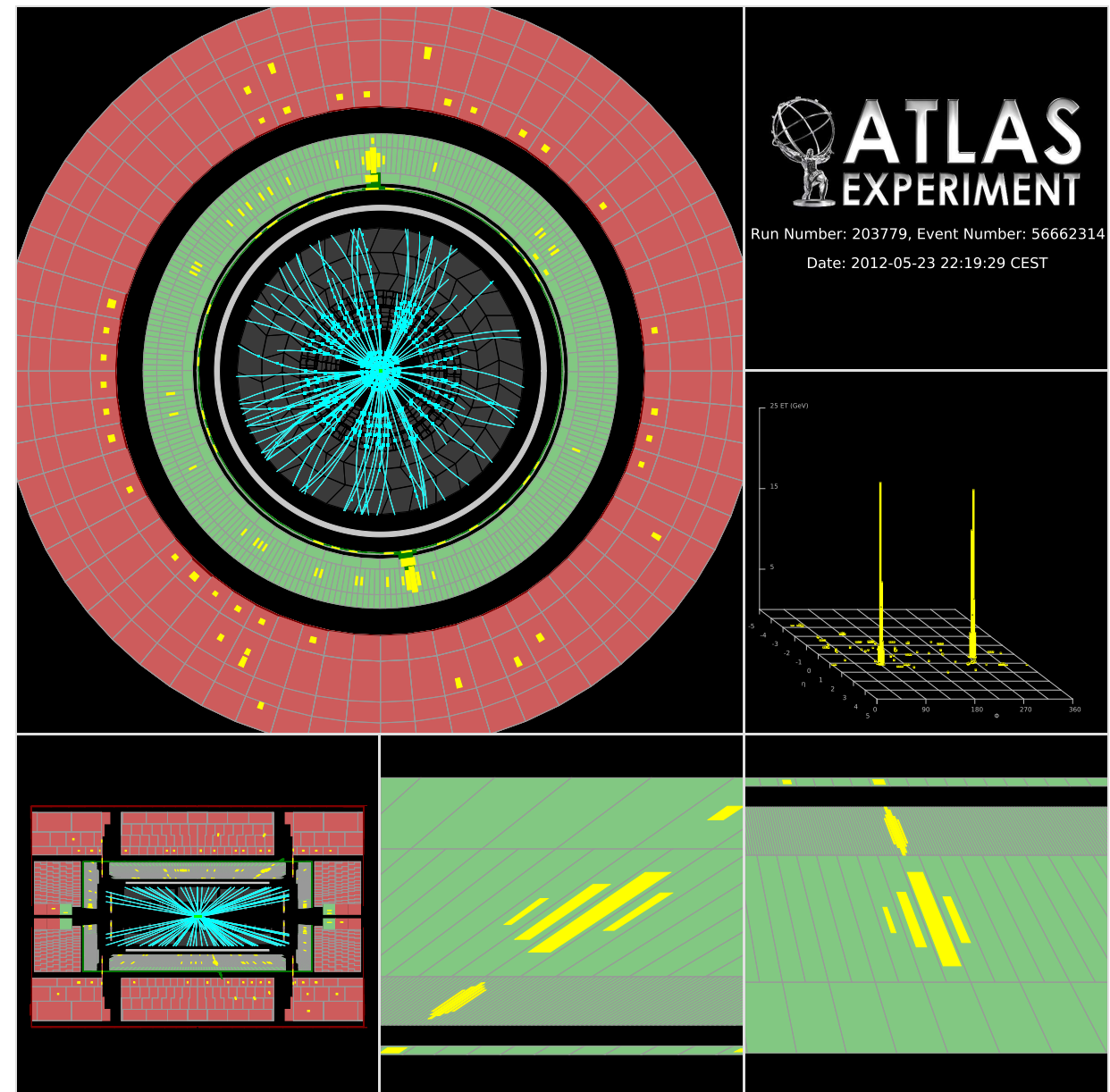
## Photon isolation



- It is essential to require the photon to be isolated. It is achieved by requiring  $E_T^{iso} \equiv \sum_i E_T^i < E_T^{\max}$  with the sum over the particles (except the photon!) inside a cone of radius  $R = 0.4$  centered on the photon in the  $\eta - \phi$  plane
- The isolation requirement suppresses the contribution of photons inside jets:  $\pi^0$  (as well as other neutral mesons) decays and the fragmentation contribution

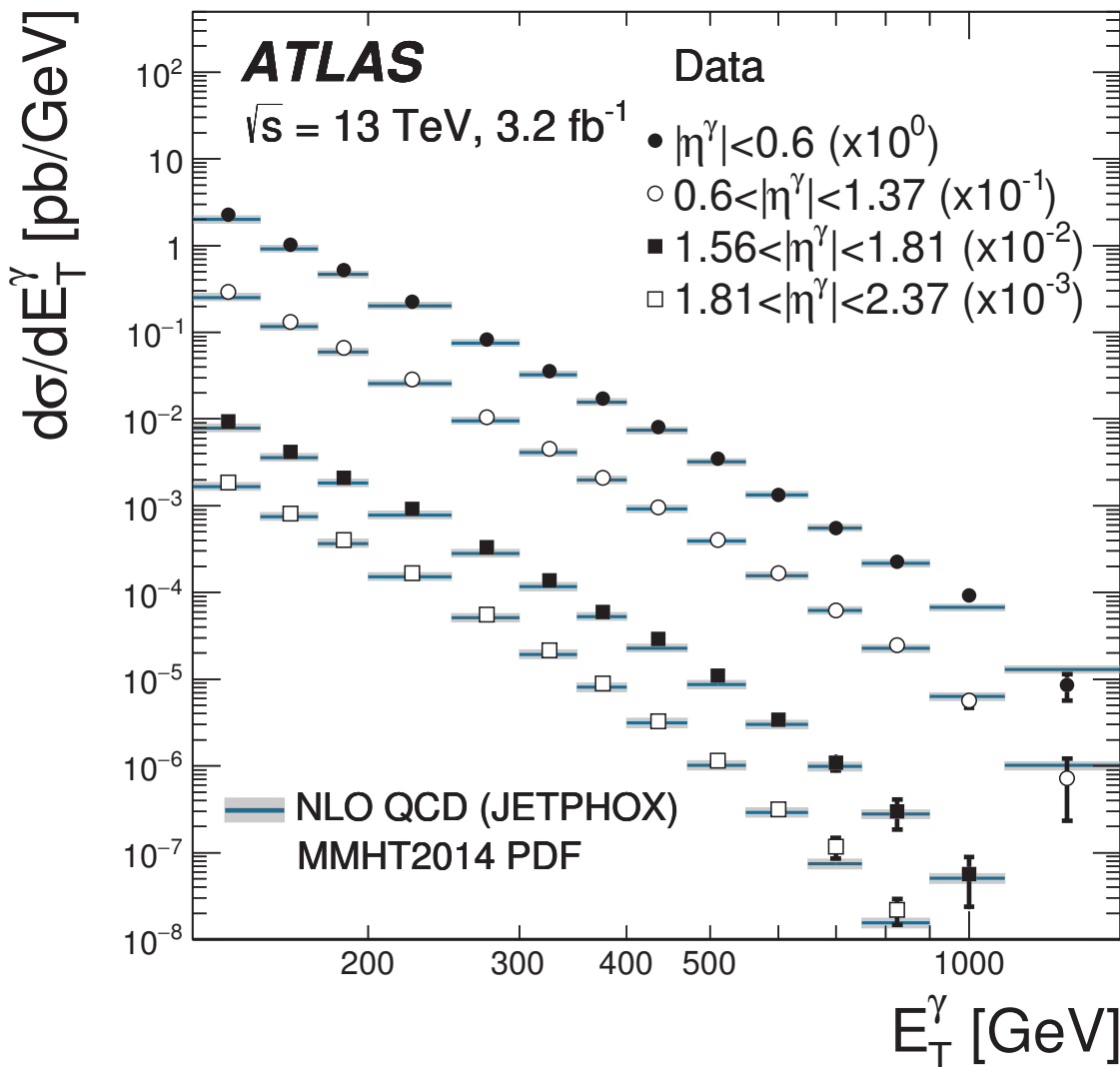
## Photon isolation in ATLAS

- $E_T^{iso}(R = 0.4)$  computed using clusters of calorimeter cells (EM and HAD) in a cone  $R = 0.4$ , excluding the contribution from the photon
- Subtraction of the leakage of the photon energy into that cone (few %)
- The underlying event and pileup (overlapping  $p\bar{p}$  interactions in the same/neighbouring bunch crossings) contribute to  $E_T^{iso}$ !  
Subtracted on event-by-event basis using the jet-area method of M. Cacciari et al
- After isolation requirement, residual background still expected



# Inclusive photon production at 13 TeV

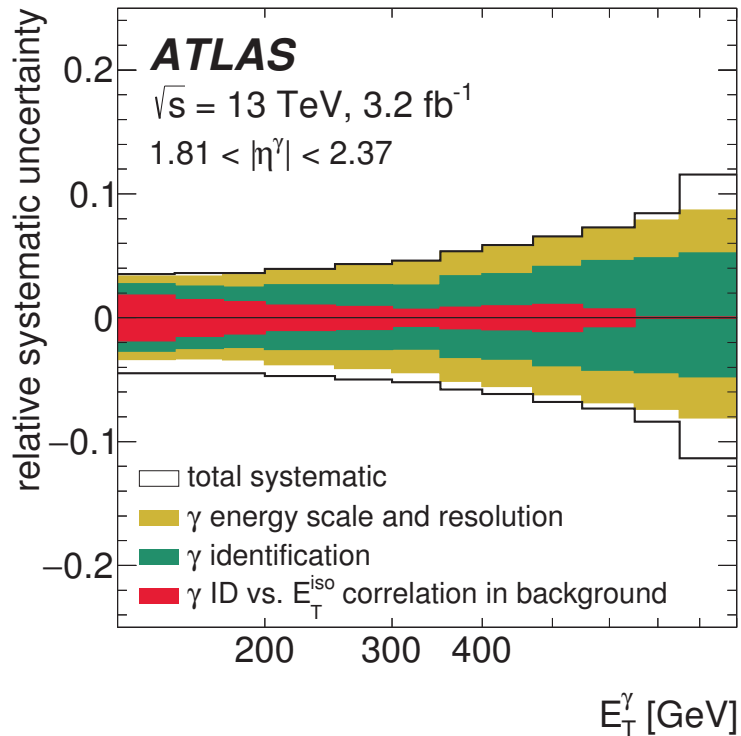
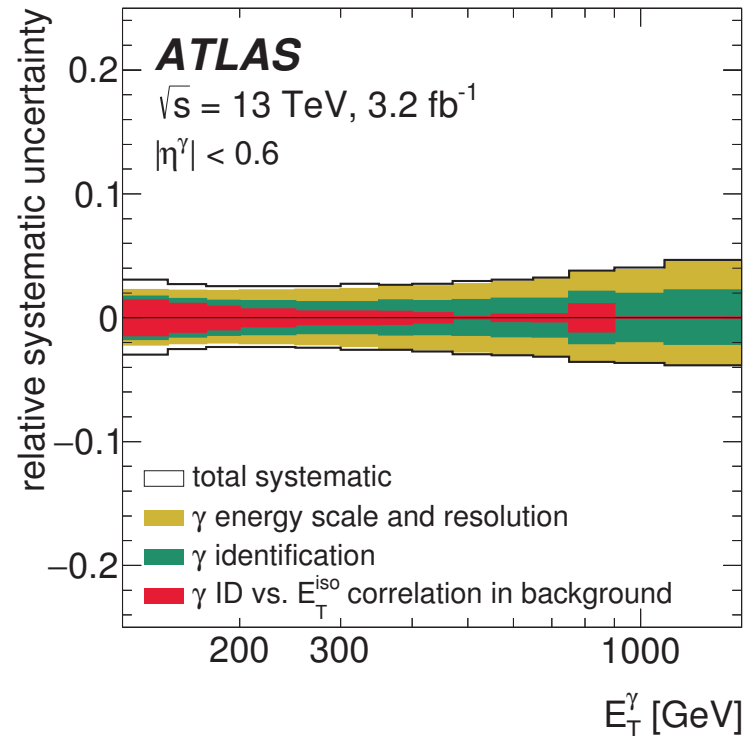
# Inclusive isolated-photon production in $pp$ collisions at $\sqrt{s} = 13$ TeV



ATLAS Coll., arXiv:1701.06882, accepted PLB

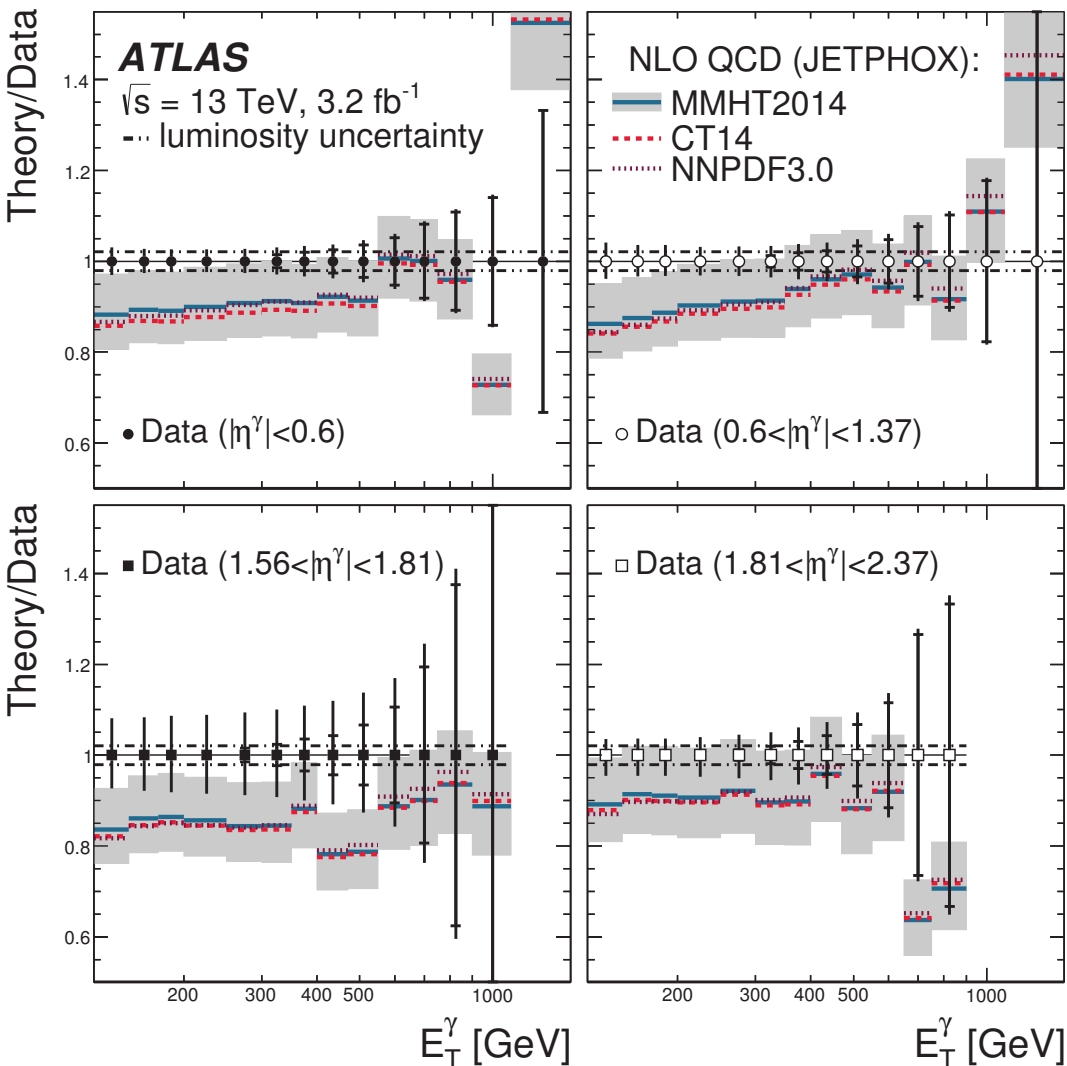
- Measurement of  $d\sigma/dE_T^\gamma$  in different ranges in  $\eta^\gamma$  for  $125 < E_T^\gamma < 1500$  GeV using  $\mathcal{L} = 3.2 \text{ fb}^{-1}$  of  $pp$  collision data at  $\sqrt{s} = 13$  TeV
- Isolation:  $E_T^{\text{iso}} < 4.2 \cdot 10^{-3} \cdot E_T^\gamma + 4.8$  GeV
- The measurement covers more than five orders of magnitude in cross section
- $d\sigma/dE_T^\gamma$  increases by a factor 2 (10) at  $E_T^\gamma = 125$  (1000) GeV with respect to at  $\sqrt{s} = 8$  TeV
- Comparison to NLO QCD predictions computed with JetPhox using the MMHT2014 PDFs

## Major experimental uncertainties



- The uncertainty on the photon energy scale dominates at high  $E_T^\gamma$ : 2–5% except for  $1.56 < |\eta^\gamma| < 1.81$ , where it is 7–18% (on the cross section)
- The uncertainty in the photon identification represents a significant contribution at low  $E_T^\gamma$ : it increases from 1–2% at 125 GeV to 2–6% at  $\sim 1$  TeV (on the cross section)
- The uncertainty in the correlation between the photon ID variables and the isolation is a significant contribution at low  $E_T^\gamma$ : typically smaller than 2% (on the cross section)

# Inclusive isolated-photon cross sections vs NLO QCD

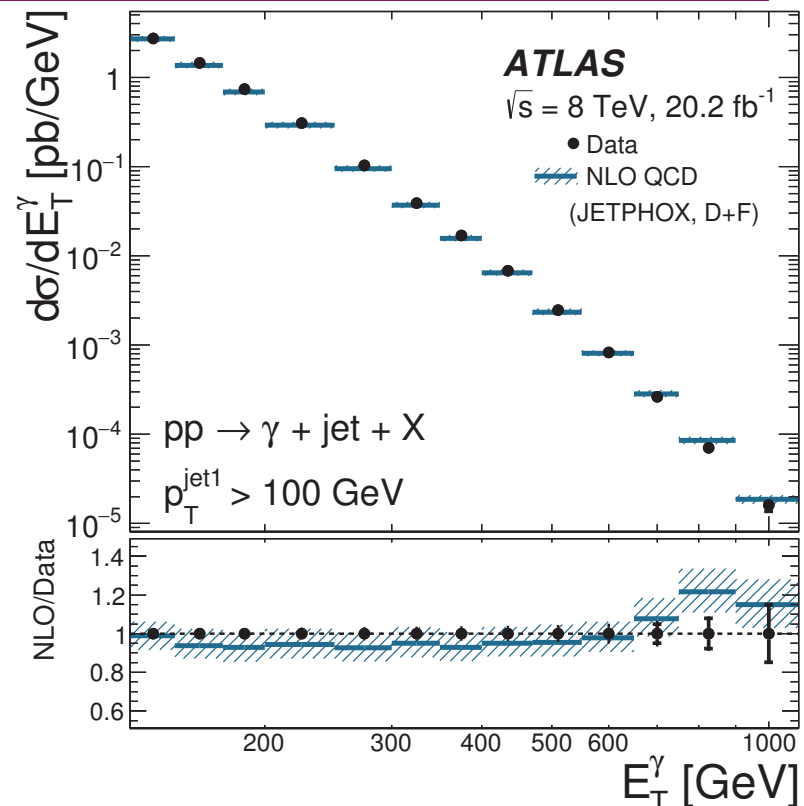


- NLO QCD predictions underestimate data by up to  $\approx 10\text{-}15\%$
- Theoretical uncertainty 10-15% much larger than experimental uncertainties
- For  $E_T^\gamma \lesssim 600$  GeV the measurements are systematically limited
- NLO QCD provides an adequate description of the data within uncertainties
- First measurement of inclusive photon production in the new kinematic regime opened by the LHC at  $\sqrt{s} = 13$  TeV
- Ready for the comparison to NNLO QCD predictions (Campbell, Ellis, Williams arXiv:1612.04333)

# Photon+jet(s) production at 8 TeV

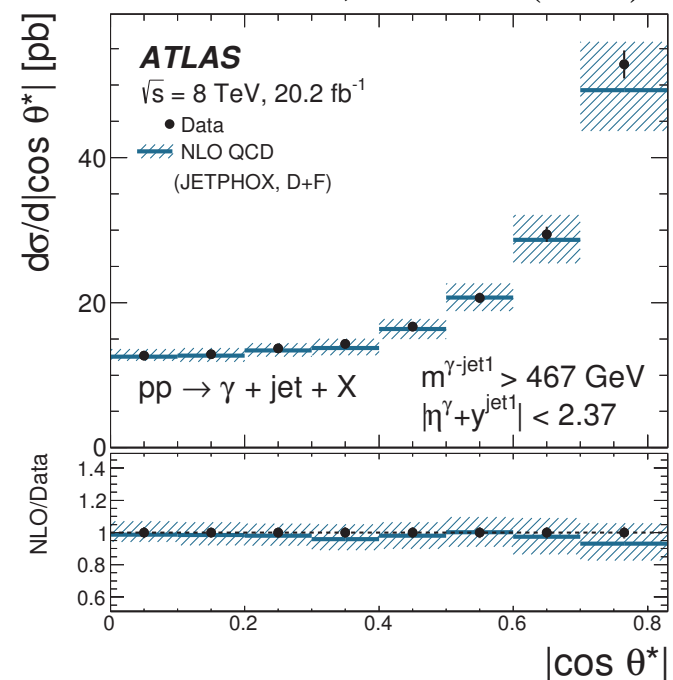
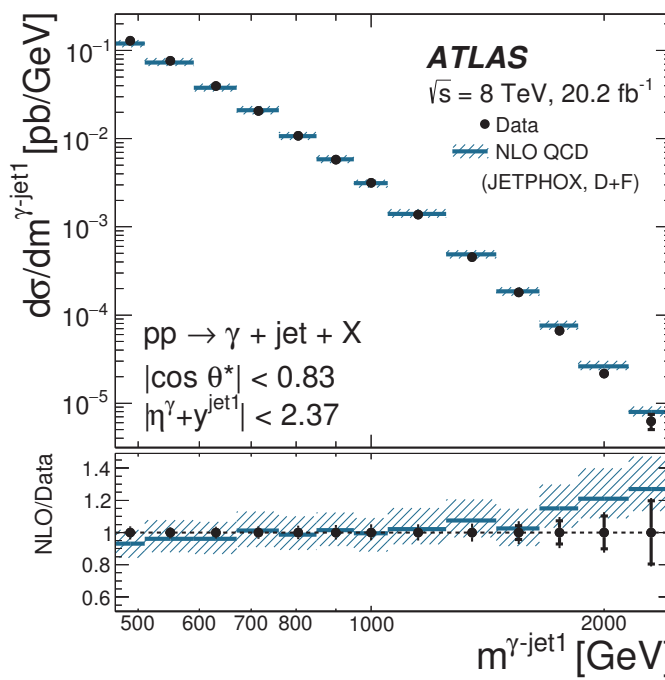
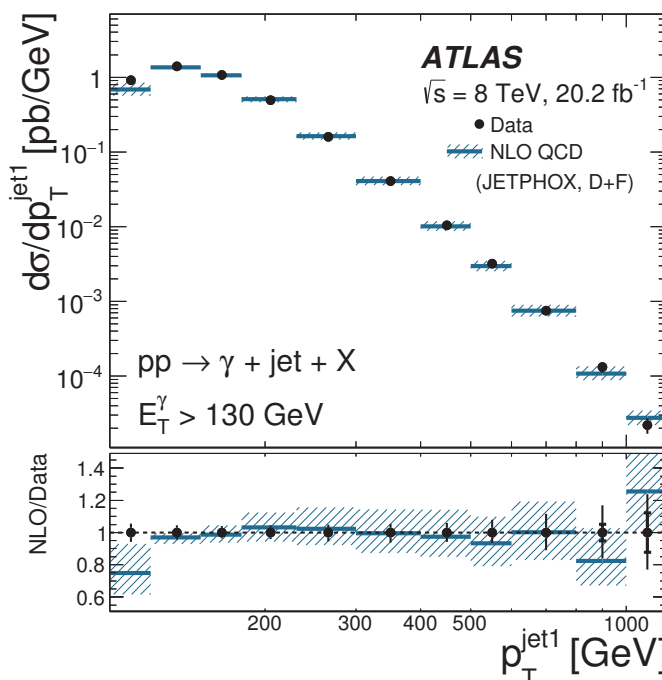
## Dynamics of $\gamma + \text{jet}$ production in $pp$ collisions at $\sqrt{s} = 8 \text{ TeV}$

- Study of the  $\gamma + \text{jet}$  dynamics by measuring the differential cross sections as functions of
  - Photon:  $E_T^\gamma$
  - Leading jet:  $p_T^{\text{jet}1}$
  - Photon+Leading jet:  $m^{\gamma-\text{jet}1}, \cos \theta^*$   
where  $\cos \theta^* = \tanh \frac{1}{2}(y^{\text{jet}1} - \eta^\gamma)$
  - θ\* = scattering angle in centre-of-mass frame for  $2 \rightarrow 2$  hard collinear scattering
- Measurements in the phase-space region defined by:  $E_T^\gamma > 130 \text{ GeV}, |\eta^\gamma| < 2.37$  (excluding the region  $1.37 < |\eta^\gamma| < 1.56$ ),  $p_T^{\text{jet}1} > 100 \text{ GeV}, |y^{\text{jet}1}| < 4.4$  (anti- $k_t$  algorithm with  $R = 0.6$ ),  $E_T^{\text{iso}} < 10 \text{ GeV}$  and  $\Delta R_{\gamma j} > 1$
- Comparison to NLO QCD calculation (JETPHOX) corrected for non-perturbative effects
- Good description of the measured  $d\sigma/dE_T^\gamma$  by the NLO QCD calculations
- Looking forward to comparison with NNLO QCD calculations (Campbell, Ellis, Williams arXiv:1703.10109)



## Dynamics of $\gamma + \text{jet}$ production in $pp$ collisions

ATLAS Coll., NPB918 (2017) 257

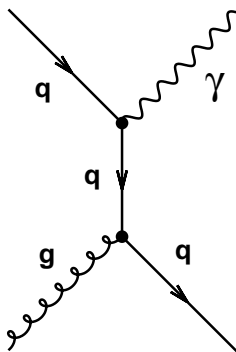


- Additional requirements for  $d\sigma/dm^{\gamma-\text{jet}1}$  and  $d\sigma/d|\cos \theta^*|$  to remove biases due to the cuts on the  $p_T$  and rapidity of the leading photon and jet:  
 $|\eta^\gamma + \eta^{\text{jet}1}| < 2.37$  ,  $|\cos \theta^*| < 0.83$  ,  $m^{\gamma-\text{jet}1} > 467 \text{ GeV}$
- In the selected (unbiased) region the angular distribution increases as  $|\cos \theta^*|$  increases
- Good description of the data by the NLO QCD calculations within the (small) experimental and theoretical uncertainties  $\Rightarrow$  validation of the description of the dynamics of  $\gamma + \text{jet}$  production in  $pp$  collisions at  $\mathcal{O}(\alpha_{em}\alpha_s^2)$

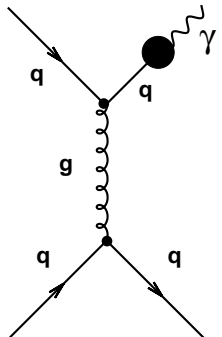
# Dynamics of $\gamma + \text{jet}$ production in $pp$ collisions

ATLAS Coll., NPB918 (2017) 257

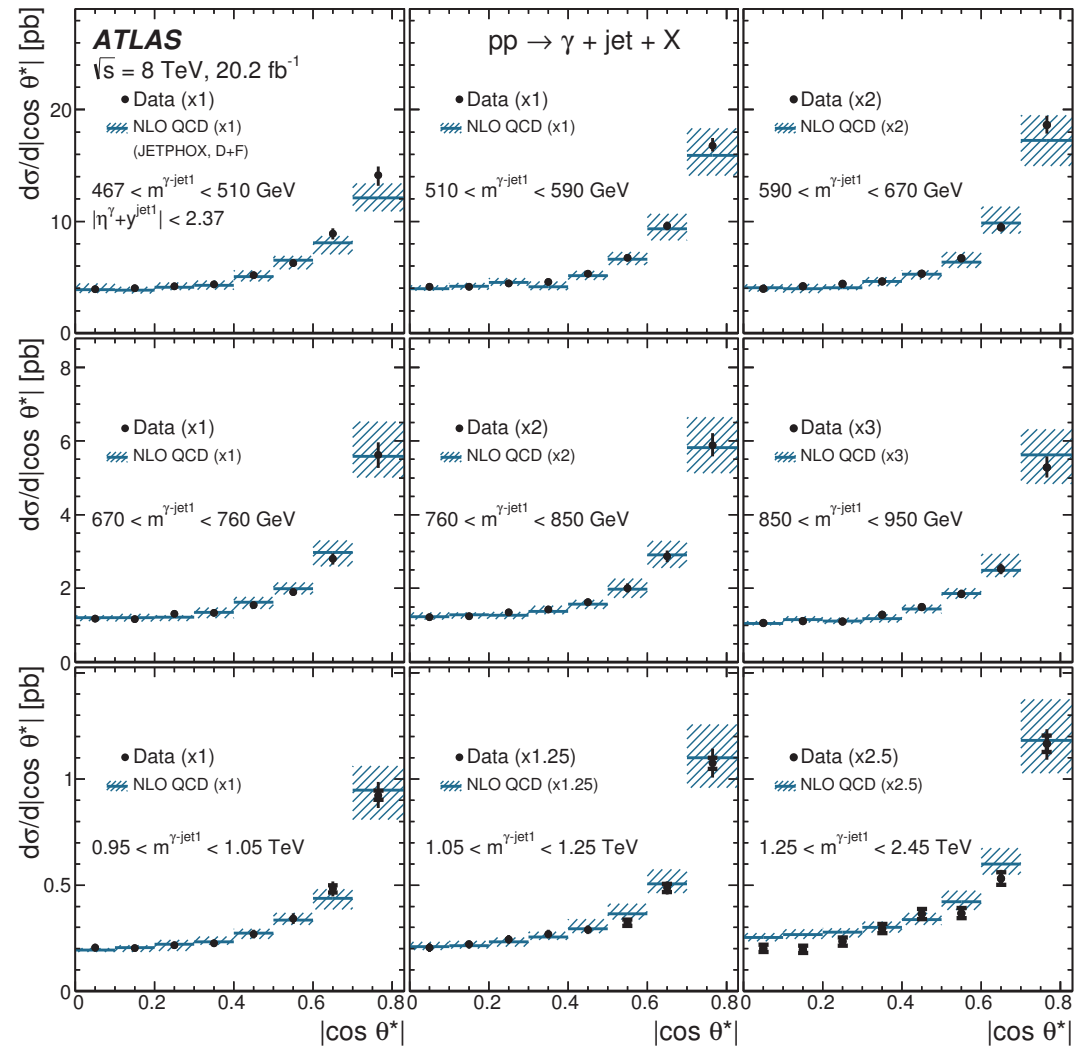
- Angular distribution  $d\sigma/d|\cos \theta^*|$   
sensitive to the spin of the exchanged  
(virtual) particle: quark(1/2) vs gluon(1)



**direct-photon process**  
 $d\sigma/d|\cos \theta^*| \sim$   
 $\sim (1 - |\cos \theta^*|)^{-1}$



**fragmentation process**  
 $d\sigma/d|\cos \theta^*| \sim$   
 $\sim (1 - |\cos \theta^*|)^{-2}$

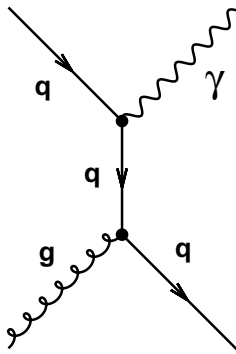


- Measured angular distribution in regions of photon-jet invariant mass  
 $\Rightarrow$  good description of the data by NLO QCD in shape and normalisation

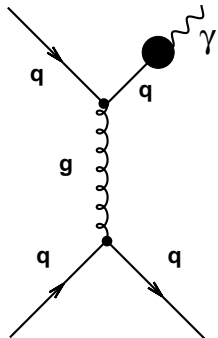
# Dynamics of $\gamma + \text{jet}$ production in $pp$ collisions

ATLAS Coll., NPB918 (2017) 257

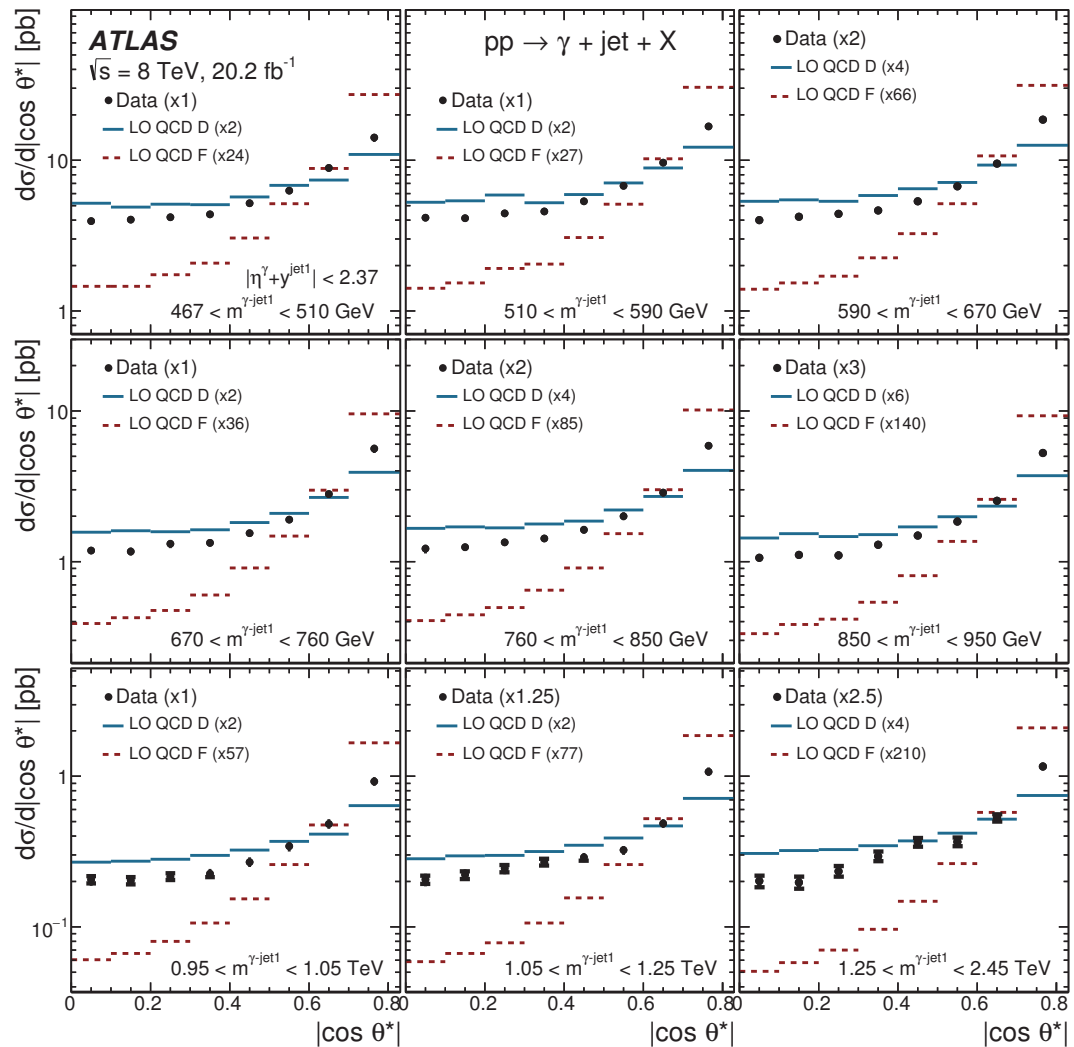
- Angular distribution  $d\sigma/d|\cos\theta^*|$   
sensitive to the spin of the exchanged  
(virtual) particle: quark(1/2) vs gluon(1)



**direct-photon process**  
 $d\sigma/d|\cos\theta^*| \sim$   
 $\sim (1 - |\cos\theta^*|)^{-1}$



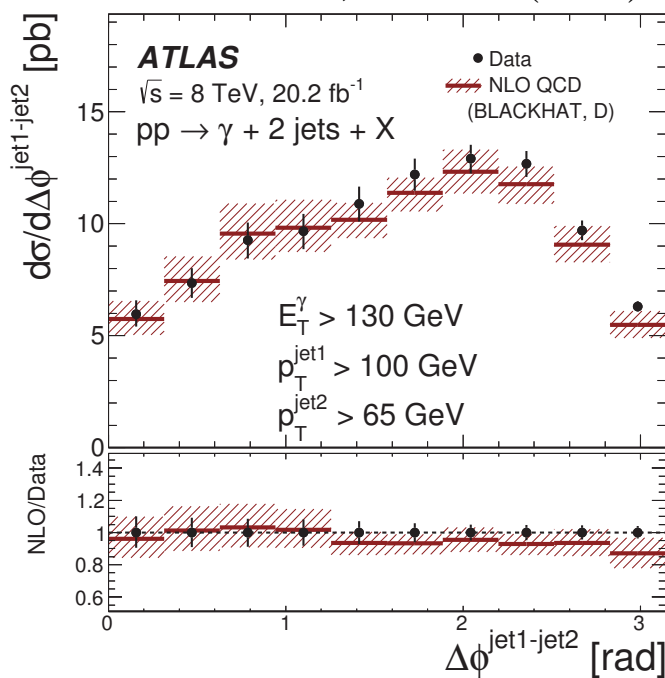
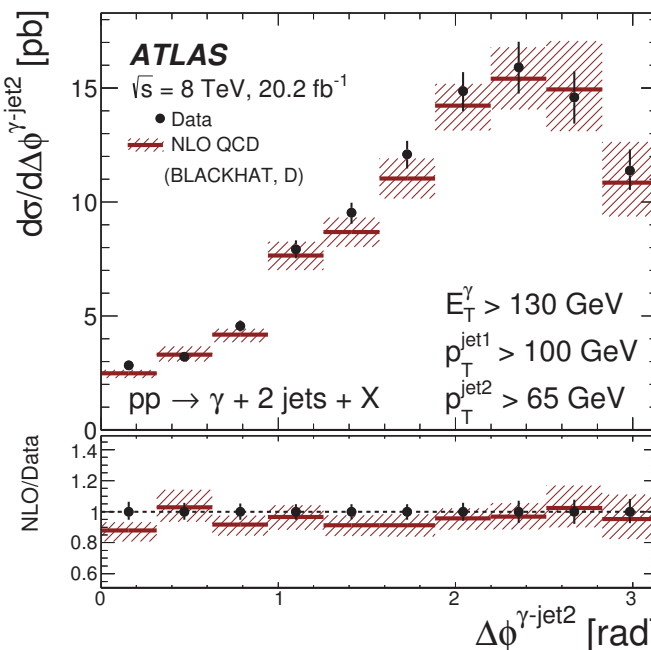
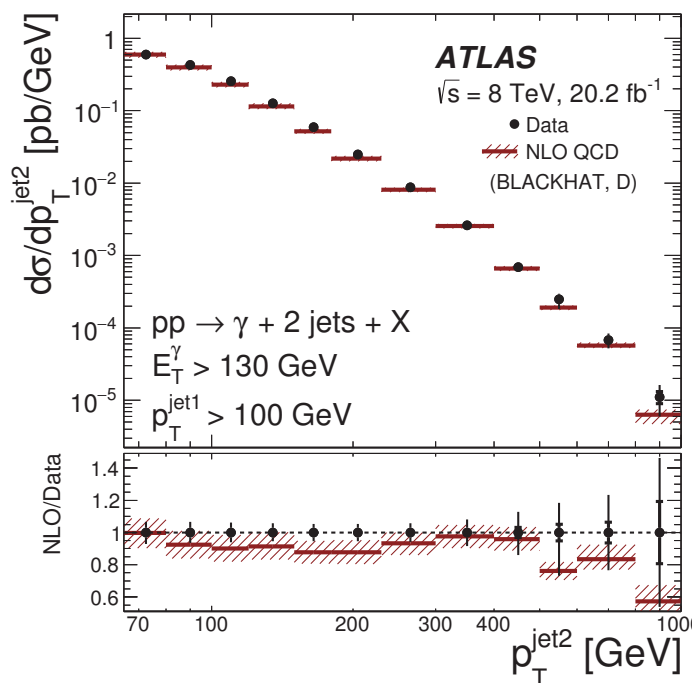
**fragmentation process**  
 $d\sigma/d|\cos\theta^*| \sim$   
 $\sim (1 - |\cos\theta^*|)^{-2}$



- Measured angular distribution closer to that of direct-photon processes than fragm.  
 $\Rightarrow$  consistent with the dominance of processes in which a virtual quark is exchanged

# Dynamics of $\gamma + 2\text{jet}$ production in $pp$ collisions

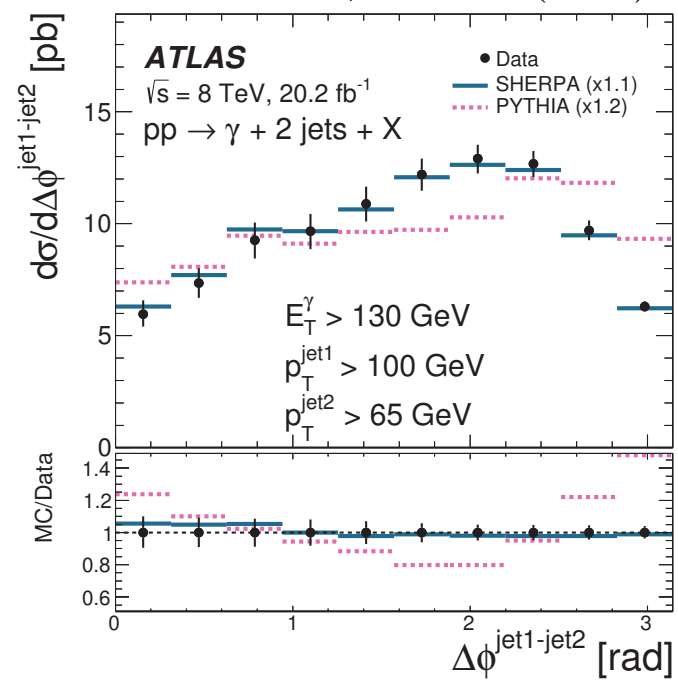
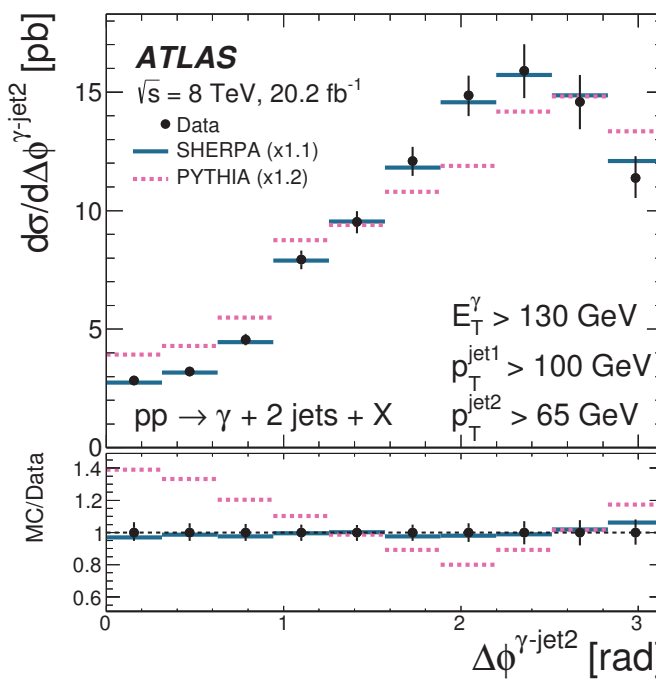
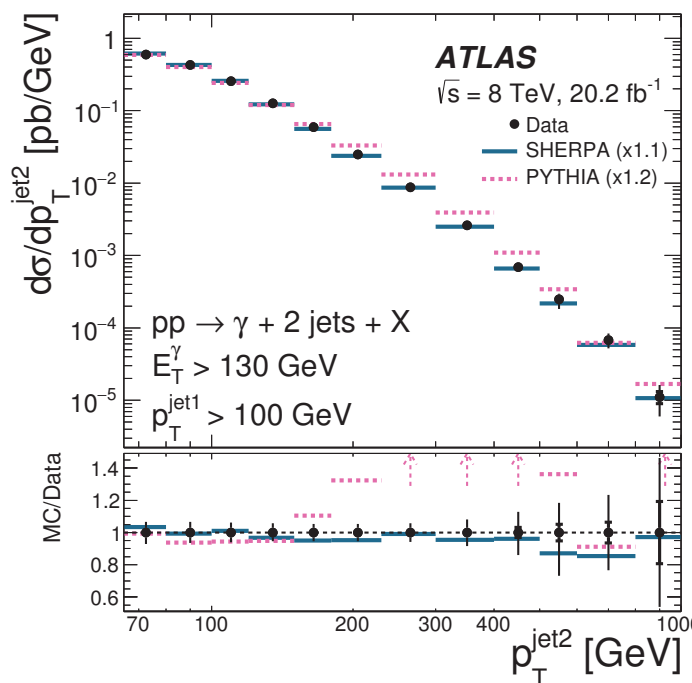
ATLAS Coll., NPB918 (2017) 257



- First measurement of  $\gamma + 2\text{jet}$  production in  $pp$  collisions at  $\sqrt{s} = 8 \text{ TeV}$ :  
 $E_T^\gamma > 130 \text{ GeV}$ ,  $p_T^{\text{jet}1} > 100 \text{ GeV}$  and  $p_T^{\text{jet}2} > 65 \text{ GeV}$
- Measurement of  $d\sigma/dp_T^{\text{jet}2}$  and angular correlations between the photon and the jets  
 $\rightarrow \Delta\phi$  between the photon and subleading jet ( $\Delta\phi^{\gamma-\text{jet}2}$ )  
 $\rightarrow \Delta\phi$  between the leading and subleading jets ( $\Delta\phi^{\text{jet}1-\text{jet}2}$ )
- Good description of the data both in shape and normalisation by the NLO QCD predictions computed with Blackhat

# Dynamics of $\gamma + 2\text{jet}$ production in $pp$ collisions

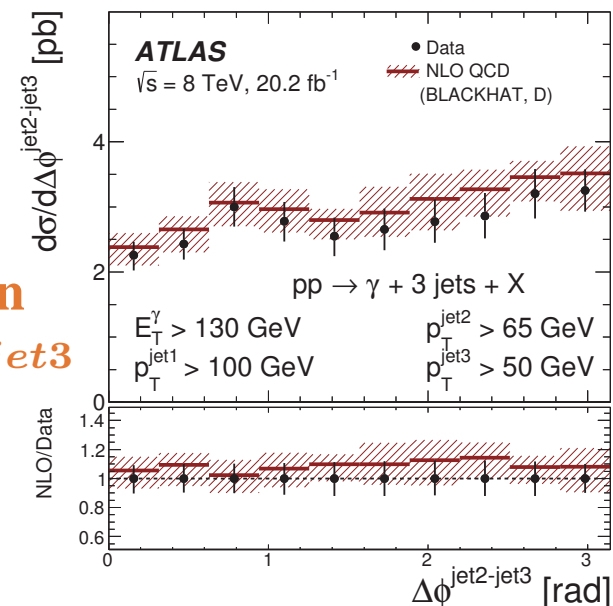
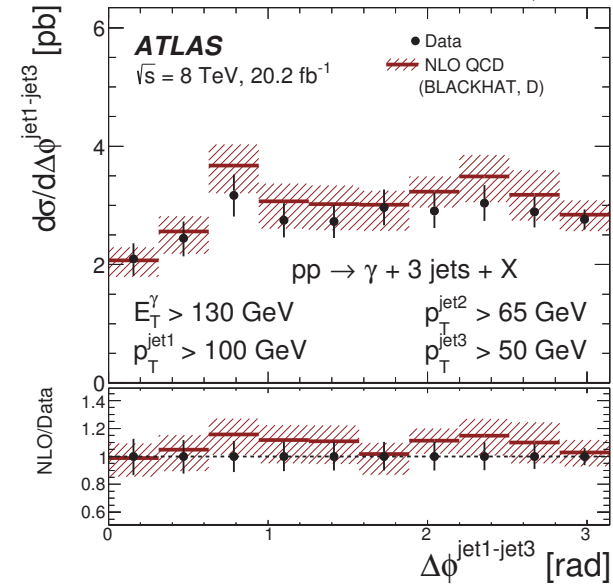
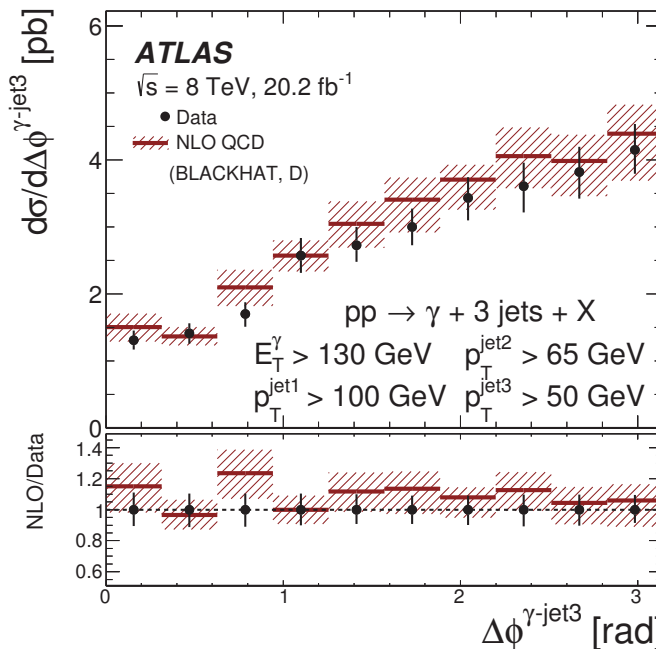
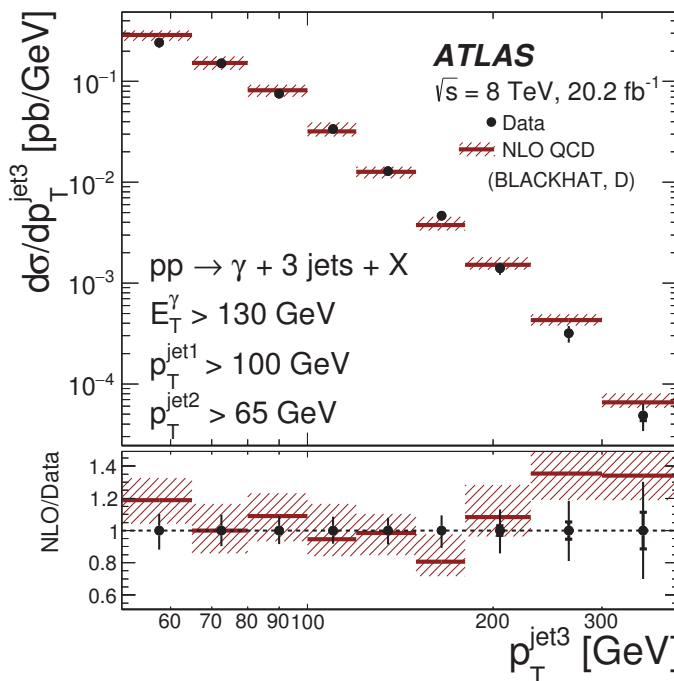
ATLAS Coll., NPB918 (2017) 257



- Comparison to the predictions of Monte Carlo generators:
  - PYTHIA:  $2 \rightarrow 2$  matrix elements plus parton showers
  - SHERPA:  $2 \rightarrow n$  ( $n = 2, \dots, 5$ ) matrix elements plus parton showers
- MC predictions normalised to data: shape comparison only
- Good description of the data by the SHERPA predictions while PYTHIA fails to describe the distribution in  $p_T^{\text{jet}2}$  and the angular correlations
- ⇒ Inclusion of higher-order tree-level ME in SHERPA improves description of data significantly

## Dynamics of $\gamma + 3\text{jet}$ production in $pp$ collisions

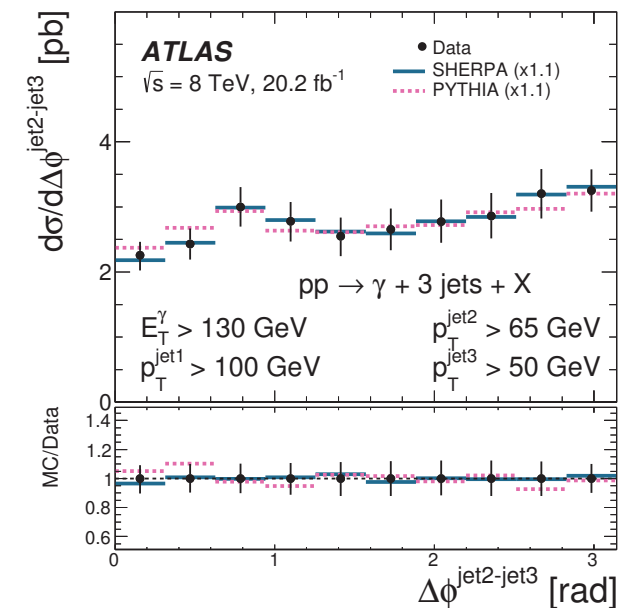
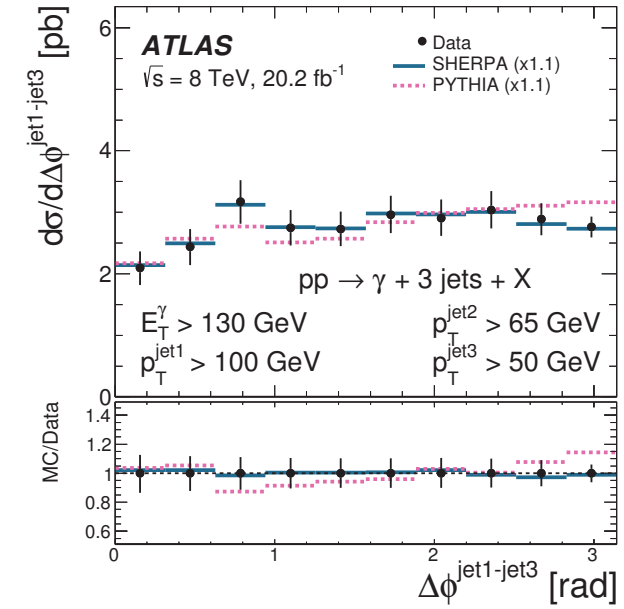
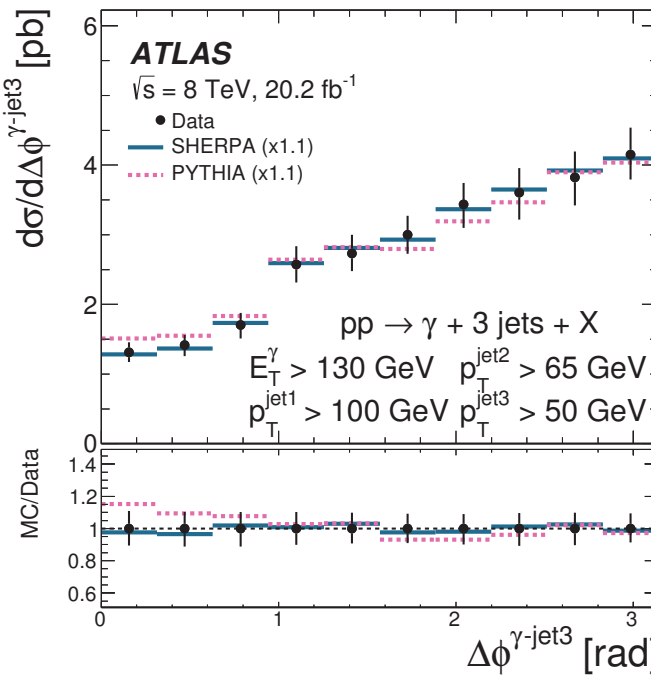
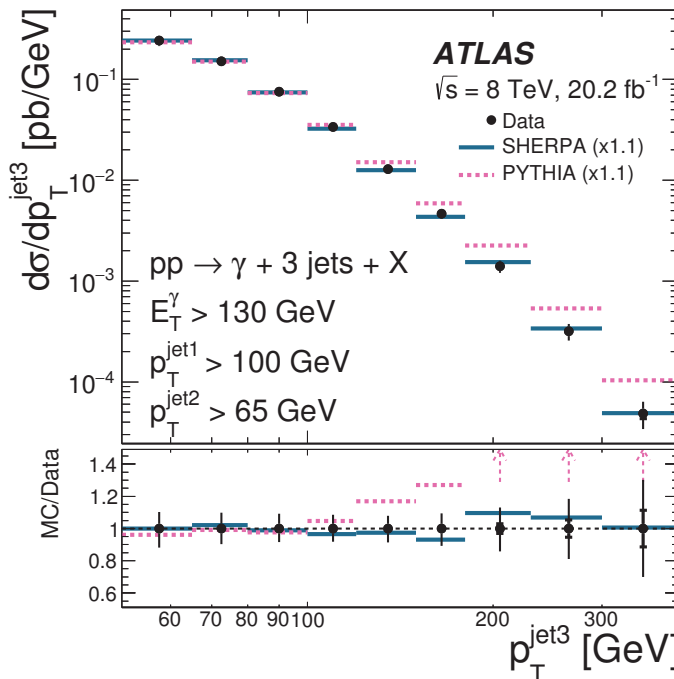
ATLAS Coll., NPB918 (2017) 257



- First measurement of  $\gamma + 3\text{jet}$  at the LHC:  $E_T^\gamma > 130 \text{ GeV}$ ,  $p_T^{\text{jet}1} > 100 \text{ GeV}$ ,  $p_T^{\text{jet}2} > 65 \text{ GeV}$  and  $p_T^{\text{jet}3} > 50 \text{ GeV}$
- Measurement of  $d\sigma/dp_T^{\text{jet}3}$  and angular correlations between the photon and the jets:  $\Delta\phi^{\gamma\text{-jet}3}$ ,  $\Delta\phi^{\text{jet}1\text{-jet}3}$ ,  $\Delta\phi^{\text{jet}2\text{-jet}3}$
- Adequate description of the data by the NLO QCD predictions computed with Blackhat

# Dynamics of $\gamma + 3\text{jet}$ production in $pp$ collisions

ATLAS Coll., NPB918 (2017) 257



- Comparison to the predictions of Monte Carlo generators of PYTHIA ( $2 \rightarrow 2$  ME+PS) and SHERPA ( $2 \rightarrow n$  ME +PS) normalised to data (shape comparison)
- Good description of the data by the SHERPA predictions while PYTHIA describes poorly the distribution in  $p_T^{\text{jet}3}$  at large values  
 $\Rightarrow$  Inclusion of higher-order tree-level ME in SHERPA improves description of data significantly

# Photon pair production at 8 TeV

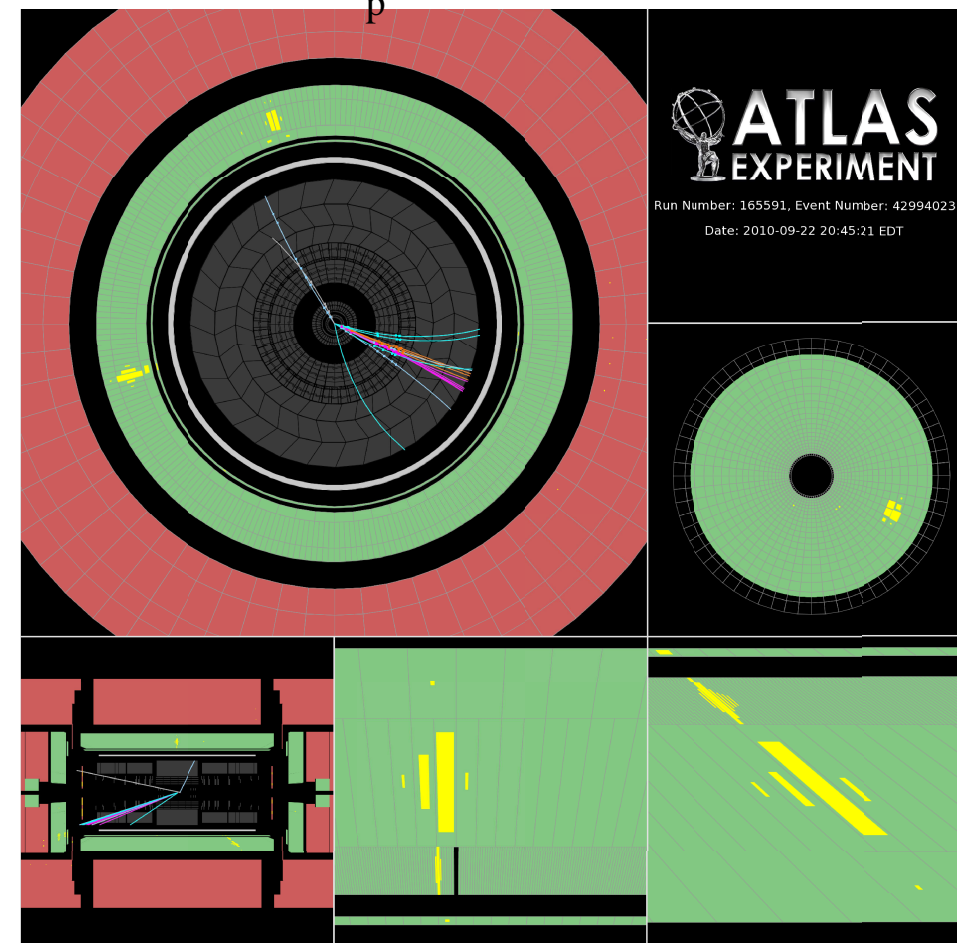
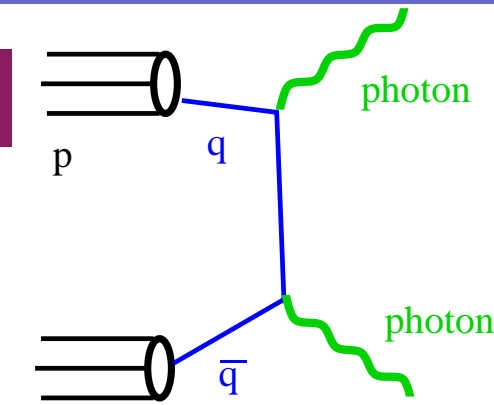
## Isolated-photon pair production in $pp$ collisions

- Measurements of the process  $pp \rightarrow \gamma\gamma + X$  with the aim of testing pQCD and understanding the irreducible background to new physics processes involving photons or  $H \rightarrow \gamma\gamma$

- Measurement of differential cross sections
  - diphoton invariant mass,  $m_{\gamma\gamma}$
  - diphoton transverse momentum,  $p_{T,\gamma\gamma}$
  - azimuthal separation in LAB frame,  $\Delta\phi_{\gamma\gamma}$
  - $\cos\theta_\eta^*$        $\rightarrow \phi_\eta^* \equiv \tan\left(\frac{\pi - \Delta\phi_{\gamma\gamma}}{2}\right) \sin\theta_\eta^*$
  - transverse component of  $\vec{p}_{T,\gamma\gamma}$  with respect to thrust axis ( $a_T$ )

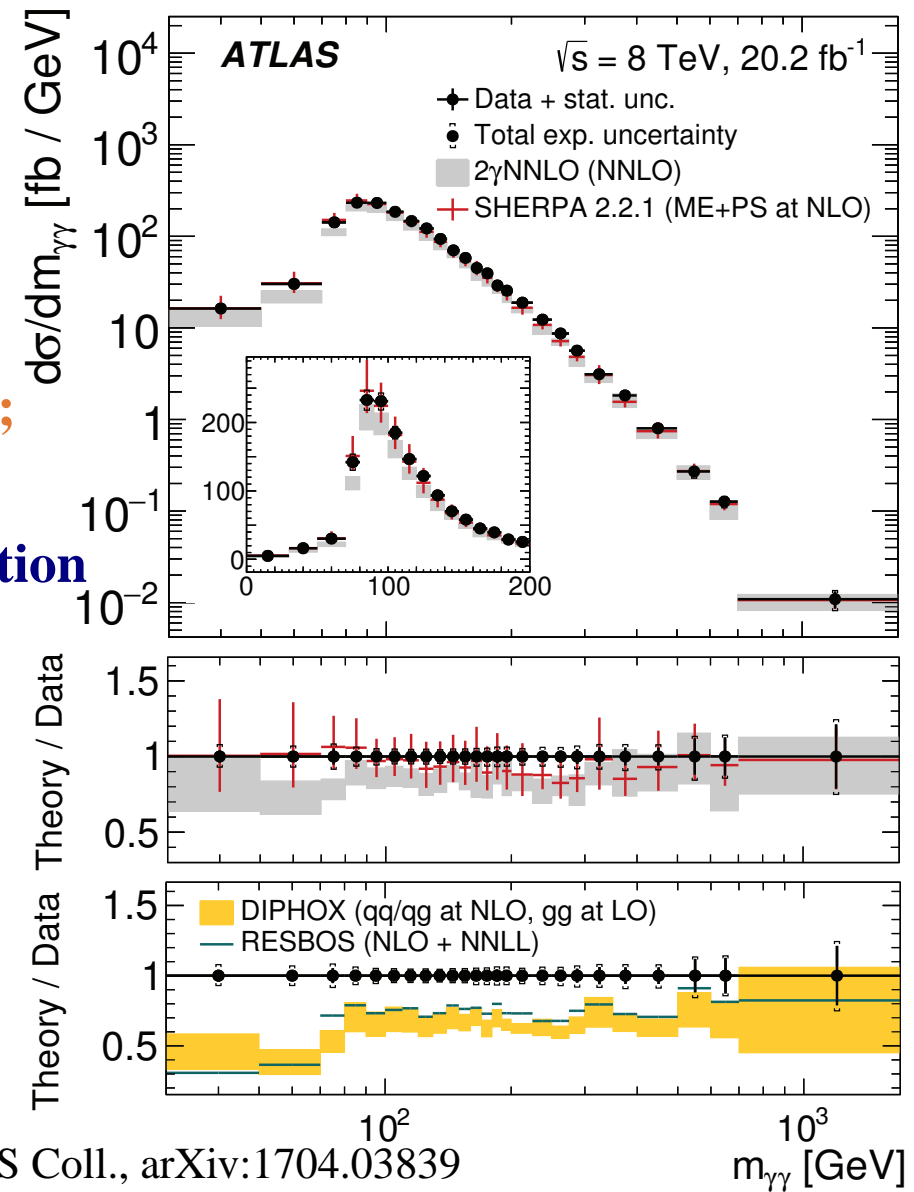
in the phase-space region defined by:

$E_T^{\gamma 1,2} > 40(30)$  GeV,  $|\eta^\gamma| < 2.37$  (excluding the region  $1.37 < |\eta^\gamma| < 1.56$ ),  $\Delta R_{\gamma\gamma} > 0.4$  and  $E_T^{iso} < 11$  GeV



# Isolated-photon pair production in $pp$ collisions at $\sqrt{s} = 8$ TeV

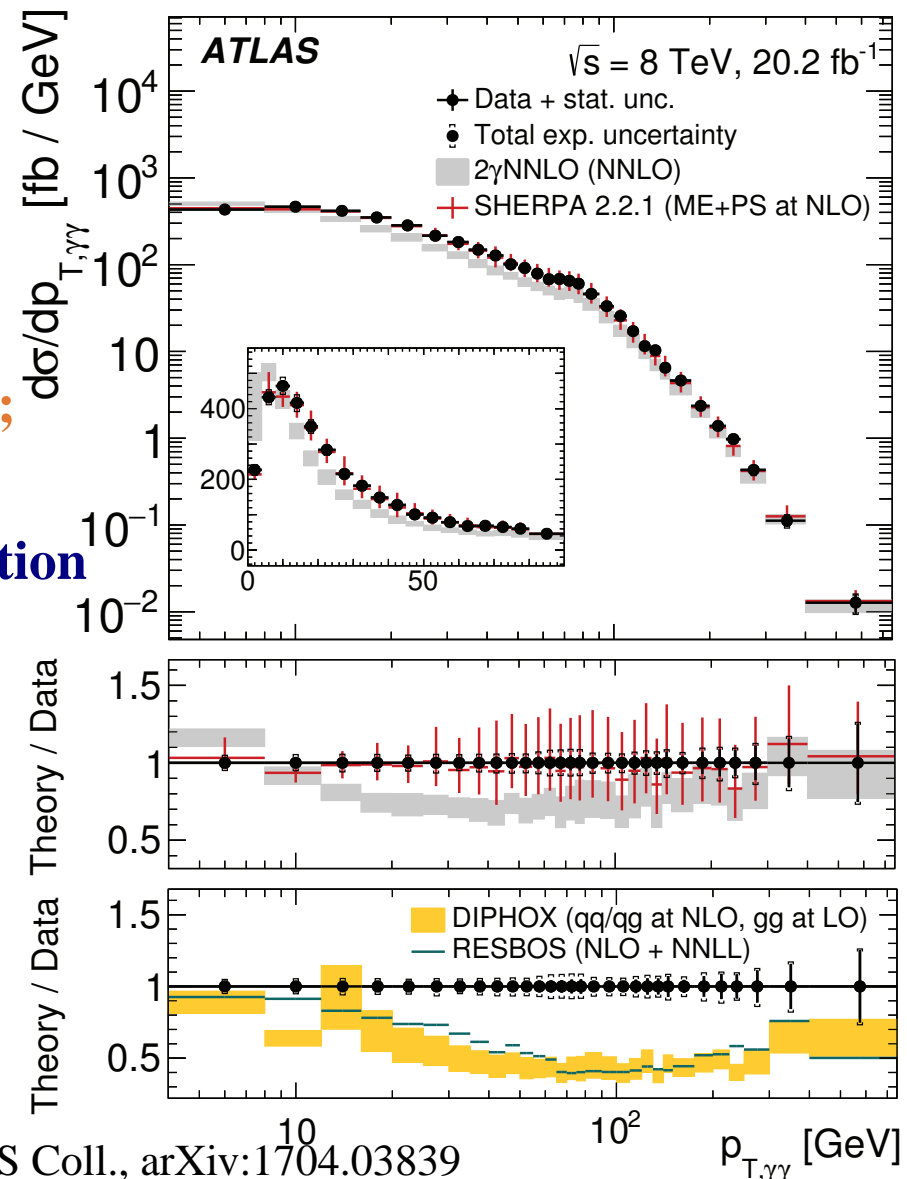
- Comparison to theoretical calculations
  - Fixed-order QCD calculations (NP corrected)
    - 2 $\gamma$ NNLO program; NNLO calculation of direct-photon contribution (no fragm.)
    - DIPHOX program; NLO calculation of direct-photon and fragmentation contributions; box diagram  $gg \rightarrow \gamma\gamma$  included
    - RESBOS program; NLO plus NNLL resummation
  - New SHERPA (v2.2.1) calculation combining
    - $\gamma\gamma$  and  $\gamma\gamma + 1p$  at NLO
    - $\gamma\gamma + 2p$  and  $\gamma\gamma + 3p$  at LO
    - parton showers
  - The small contribution from  $H \rightarrow \gamma\gamma$  is neglected
- ⇒ SHERPA prediction in agreement with data



ATLAS Coll., arXiv:1704.03839

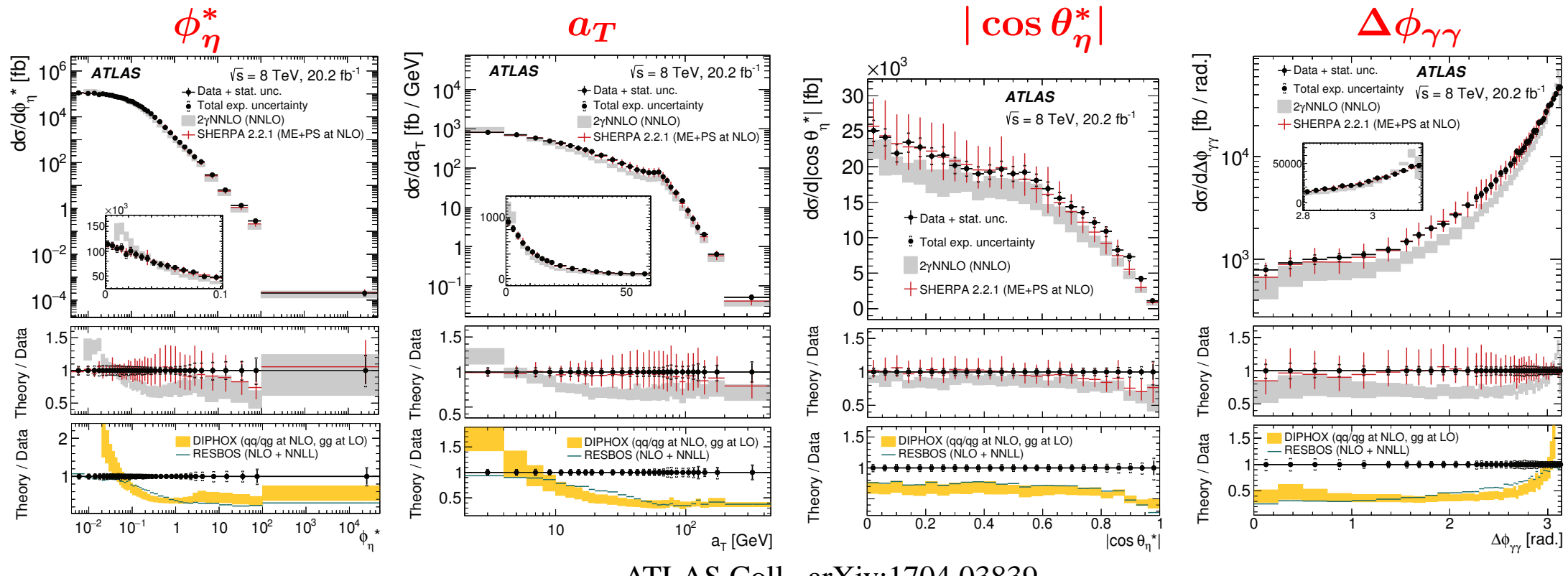
## Isolated-photon pair production in $pp$ collisions at $\sqrt{s} = 8$ TeV

- Comparison to theoretical calculations
- Fixed-order QCD calculations (NP corrected)
  - 2 $\gamma$ NNLO program; NNLO calculation of direct-photon contribution (no fragm.)
  - DIPHOX program; NLO calculation of direct-photon and fragmentation contributions; box diagram  $gg \rightarrow \gamma\gamma$  included
  - RESBOS program; NLO plus NNLL resummation
- New SHERPA (v2.2.1) calculation combining
  - $\gamma\gamma$  and  $\gamma\gamma + 1p$  at NLO
  - $\gamma\gamma + 2p$  and  $\gamma\gamma + 3p$  at LO
  - parton showers
- The small contribution from  $H \rightarrow \gamma\gamma$  is neglected
- ⇒ SHERPA prediction in agreement with data



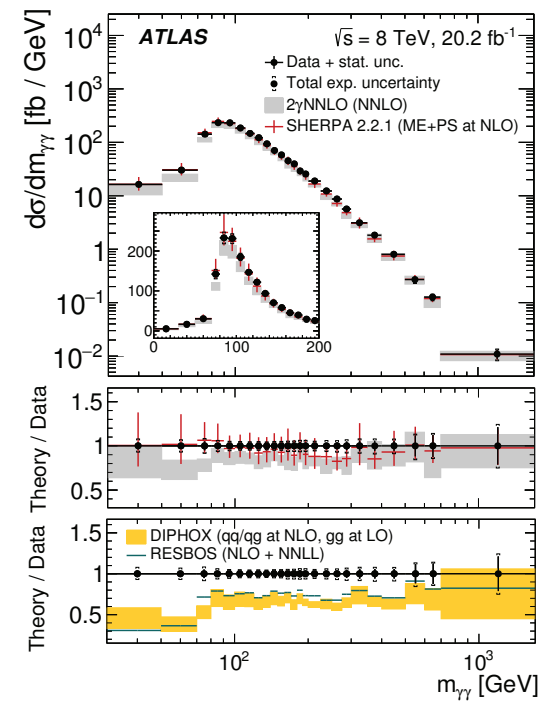
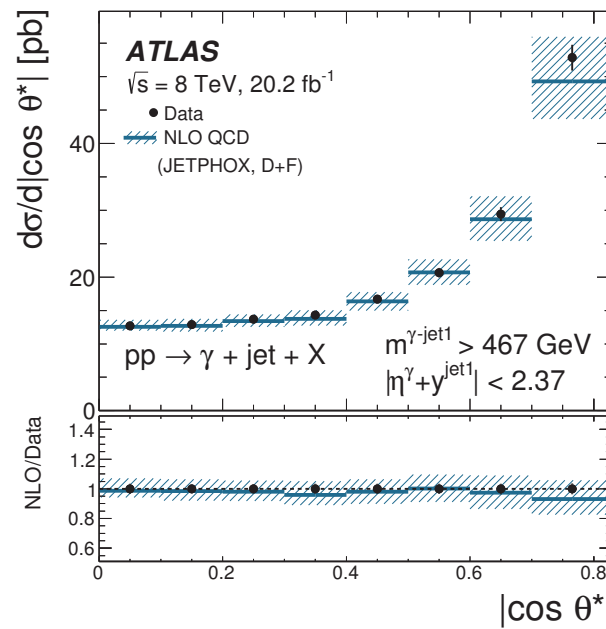
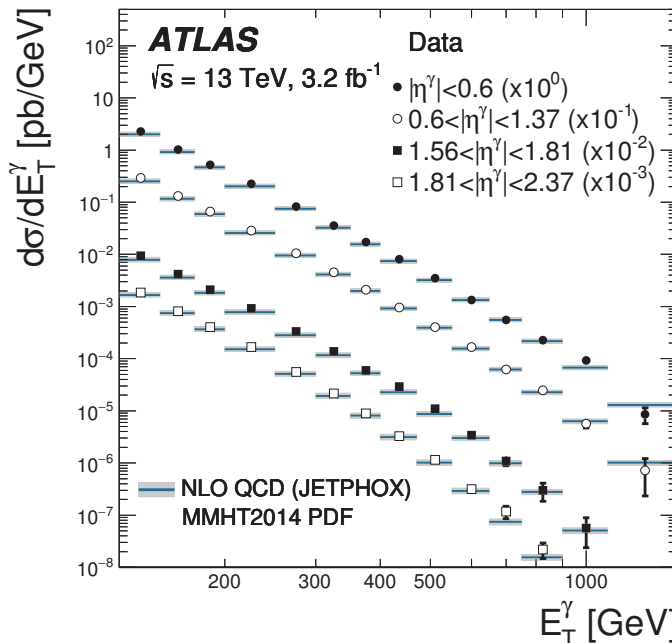
ATLAS Coll., arXiv:1704.03839

# Isolated-photon pair production in $pp$ collisions at $\sqrt{s} = 8$ TeV



- $\Delta\phi_{\gamma\gamma} \sim \pi$  or at low values of  $p_{T,\gamma\gamma}$ ,  $a_T$  and  $\phi_\eta^*$  (soft gluon resummation important): **RESBOS** and **SHERPA** do well
- NLO QCD calculations without higher order terms (**DIPHOX**, **RESBOS**) are insufficient
- NNLO corrections ( $2\gamma$ NNLO) improve the description, but still insufficient
- **SHERPA** predictions agree with the data

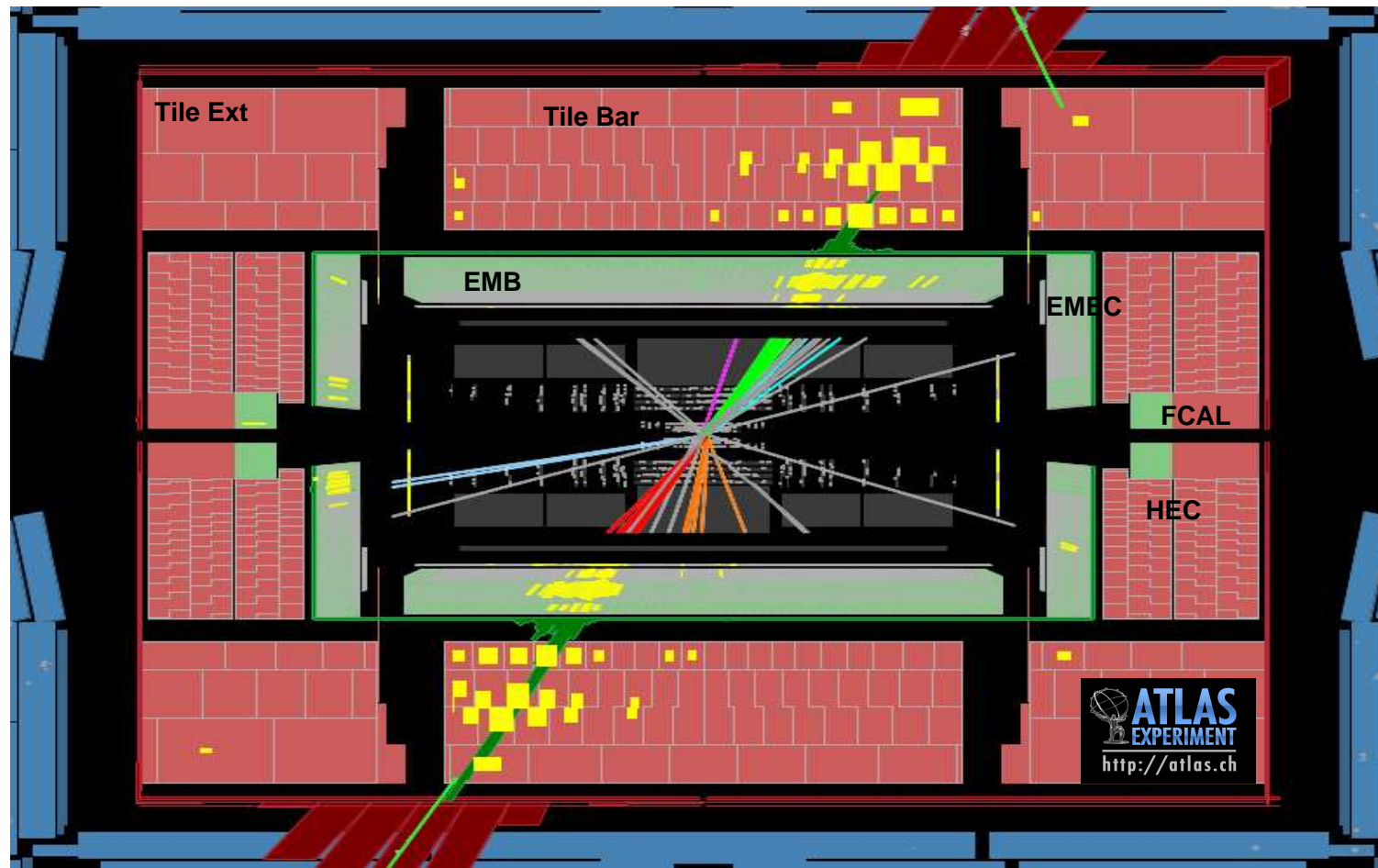
## Summary



- Exploration of isolated photon production in  $pp$  collisions up to  $E_T^\gamma \sim 1 \text{ TeV}$
- Additional experimental information on the gluon density in the proton
- Measurement of the dynamics of photon+jet(s) and diphoton production
- Understanding (in pQCD) the background to Higgs into  $\gamma\gamma$
- Overall, perturbative QCD succeeds in describing the data!

**Backup**

## The ATLAS detector



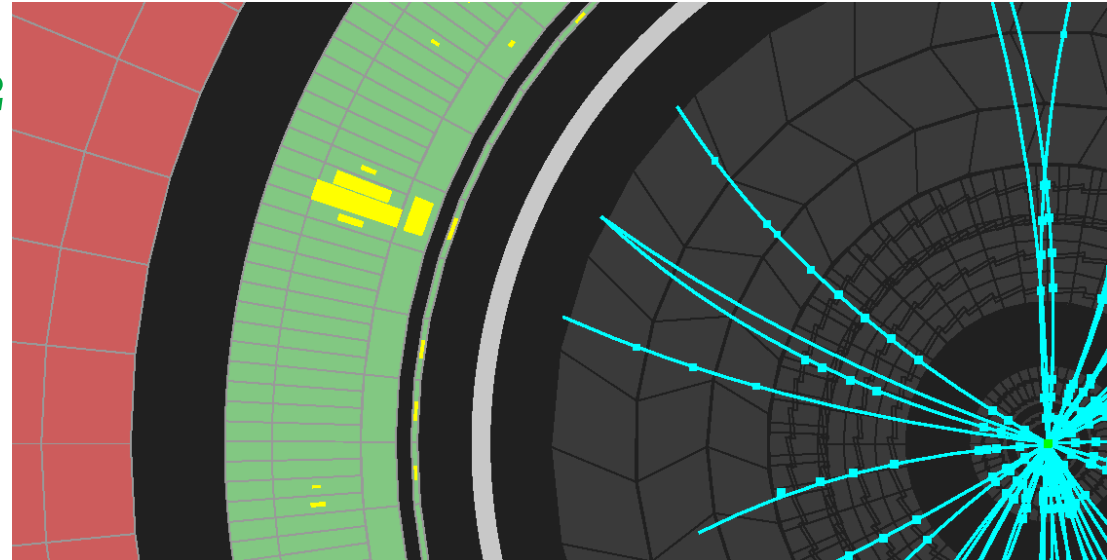
- Inner detector (ID): tracking and particle identification in  $|\eta| < 2.5$
- Calorimeters: electromagnetic (LAr) → barrel  $|\eta| < 1.475$ , endcap  $1.375 < |\eta| < 3.2$ , forward  $3.1 < |\eta| < 4.9$ ; hadronic (scintillator/steel, LAr/Cu, LAr/W) → barrel  $|\eta| < 0.7$  extended barrel  $0.8 < |\eta| < 1.7$ , endcap  $1.5 < |\eta| < 3.2$  and forward  $3.1 < |\eta| < 4.9$

## Photon reconstruction in the ATLAS LAr Calorimeter

- Layout of the ATLAS electromagnetic calorimeter (Lead-liquid Argon)

- barrel section,  $|\eta| < 1.475$
- two end-cap sections,  $1.375 < |\eta| < 3.2$
- three longitudinal layers

- First layer: high granularity in  $\eta$  direction, width 0.003-0.006 (except for  $1.4 < |\eta| < 1.5$  and  $|\eta| > 2.4$ )
- Second layer: collects most of the energy, granularity  $0.025 \times 0.025$  in  $\eta \times \phi$
- Third layer: used to correct for leakage

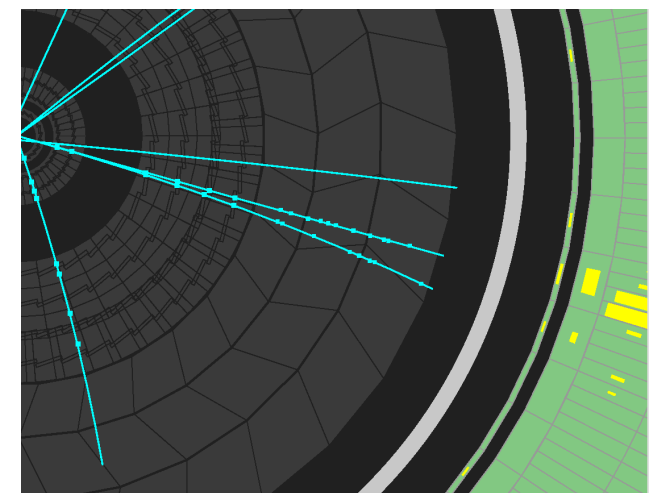


- Cluster of EM cells without matching track:

- “unconverted” photon candidate

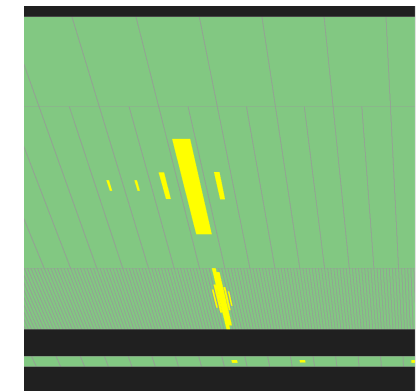
- Cluster of EM cells matched to pairs of tracks (from reconstructed conversion vertices in the inner detector) or matched to a single track consistent with originating from a photon conversion

- “converted” photon candidate



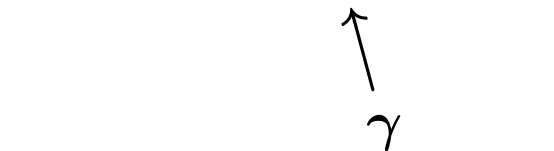
## Photon identification in the ATLAS LAr Calorimeter

- To discriminate signal vs background: shape variables from the lateral and longitudinal energy profiles of the shower in the calorimeters; “loose” and “tight” identification criteria.



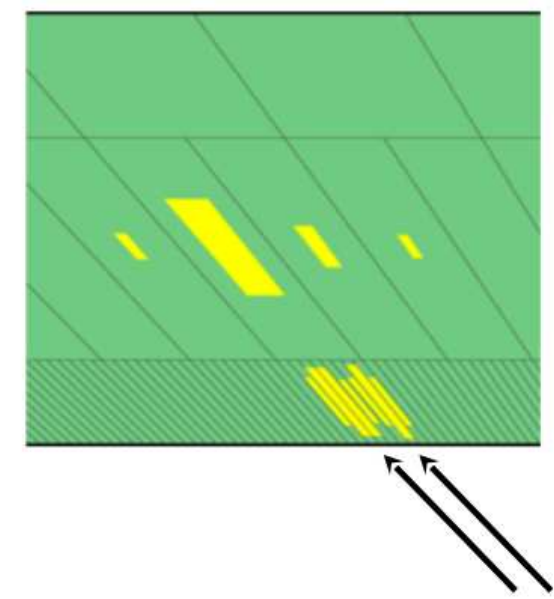
- “Loose” identification criteria:

- leakage  $R_{had} = E_T^{had}/E_T$  (1st layer hadronic calorimeter)
- $R_\eta = E_{3 \times 7}^{S2}/E_{7 \times 7}^{S2}$ ; S2=second layer of EM calorimeter
- RMS width of the shower in  $\eta$  direction in S2



- “Tight” identification criteria:

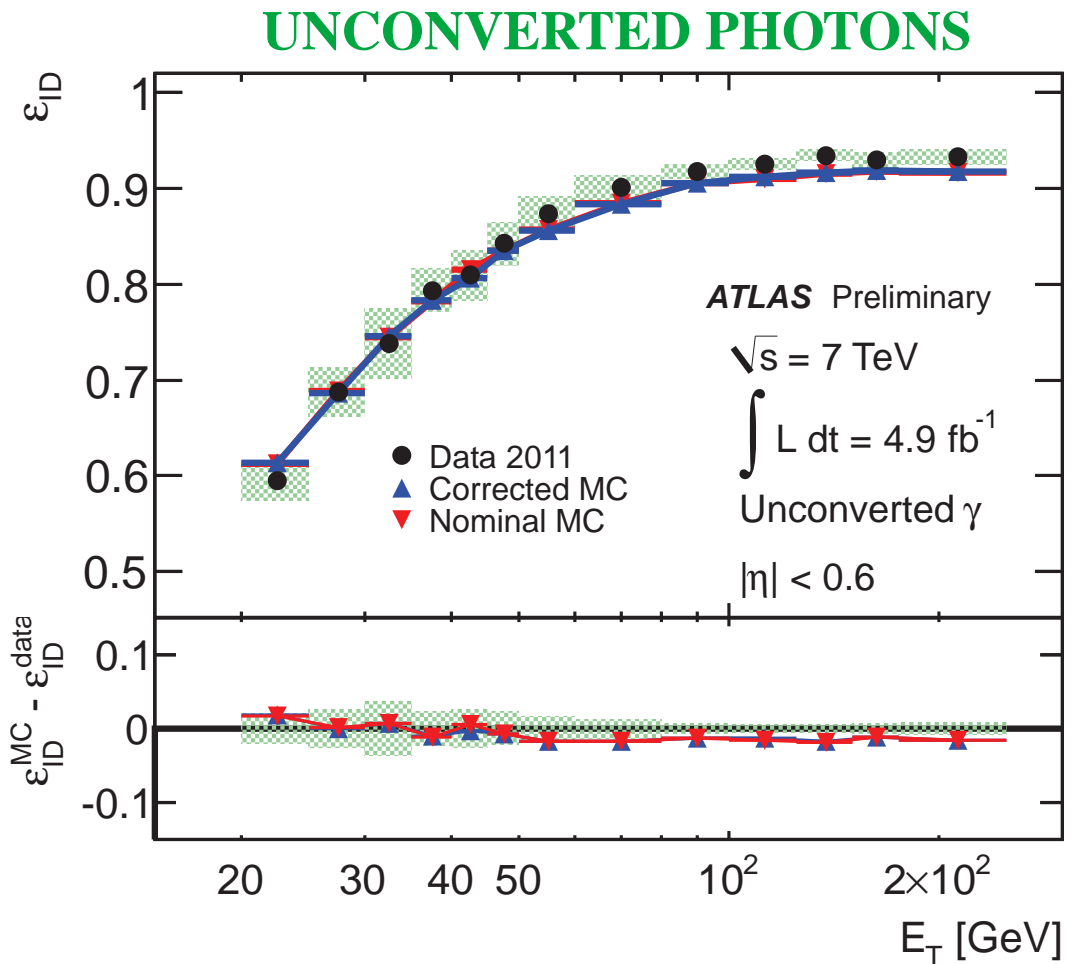
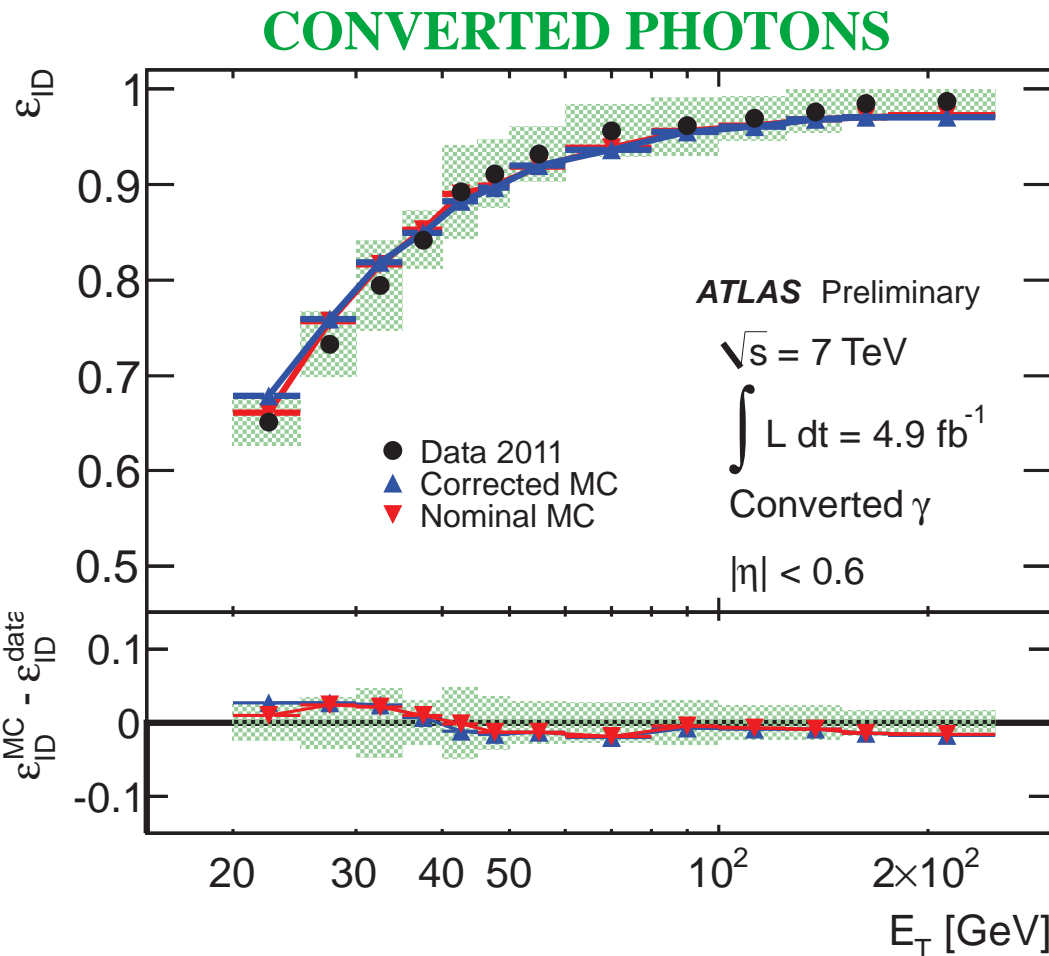
- the requirements applied in “Loose” are tightened
- $R_\phi = E_{3 \times 3}^{S2}/E_{3 \times 7}^{S2}$   
and shower shapes in the first layer (to discriminate single-photon showers from overlapping nearby showers, such as  $\pi^0 \rightarrow \gamma\gamma$ )
- e.g. asymmetry between the 1st and 2nd maxima in the energy profile along  $\eta$  ( $S1$ )



$$\pi^0 \rightarrow \gamma\gamma$$

## Photon identification efficiency

ATLAS Coll., ATLAS-CONF-2012-123

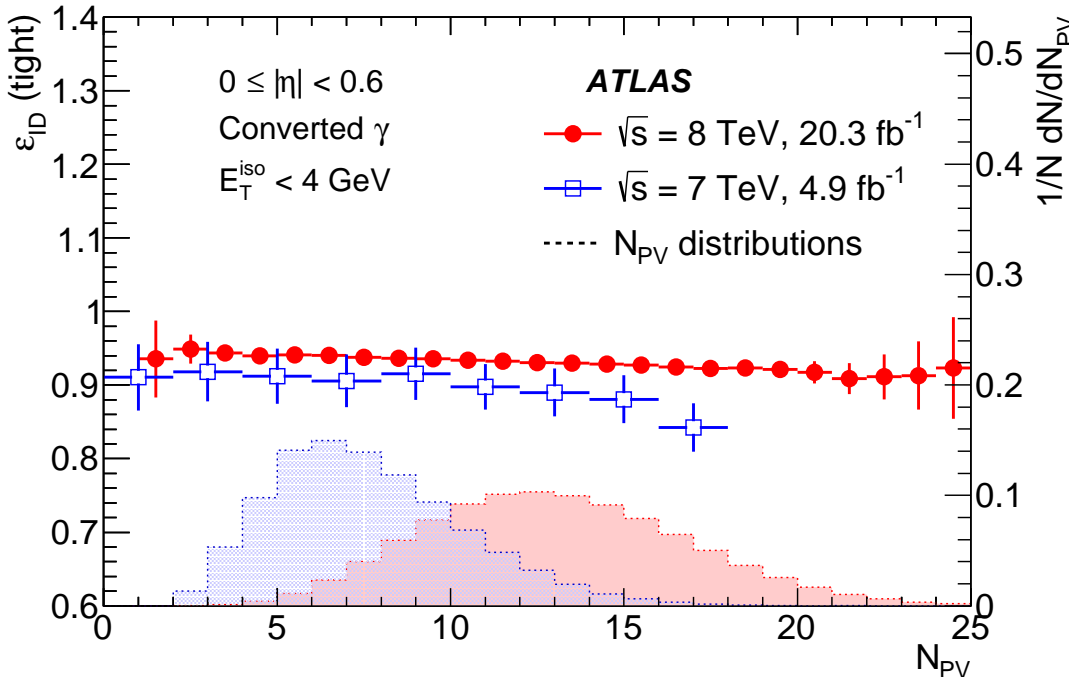


- Data-driven measurements of photon identification efficiency for converted and unconverted photons (radiative  $Z$  decays, extrapolation from  $e^\pm$  and matrix method) compared to estimations based on Monte Carlo simulations

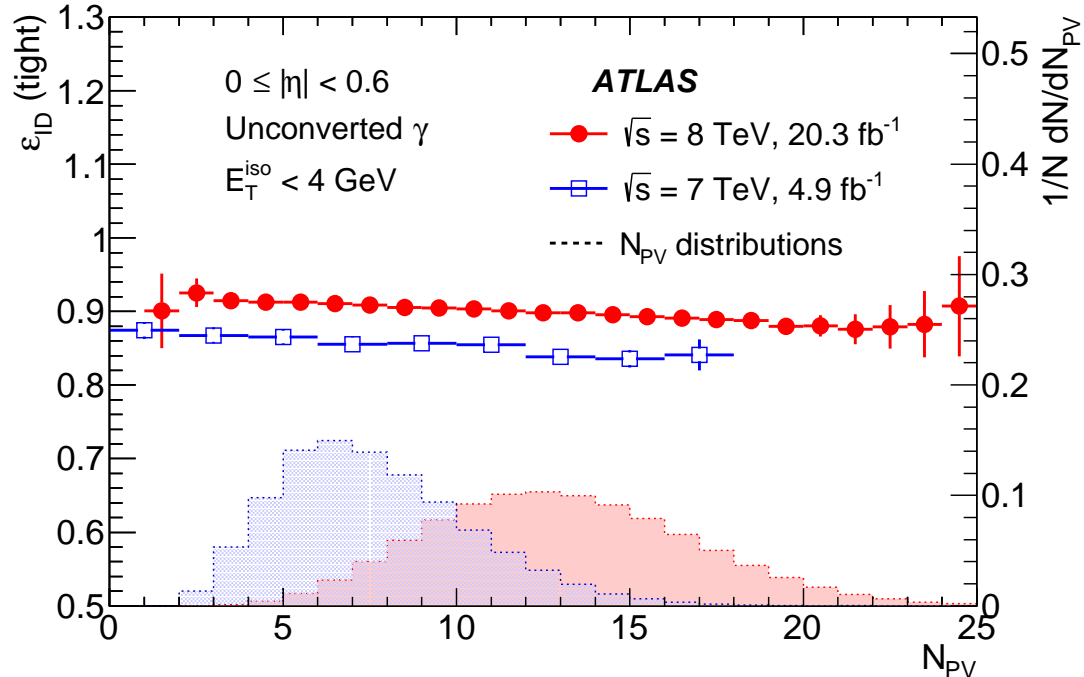
# Photon identification efficiency vs pile-up

ATLAS Coll., EPJC 76 (2016) 666

## CONVERTED PHOTONS



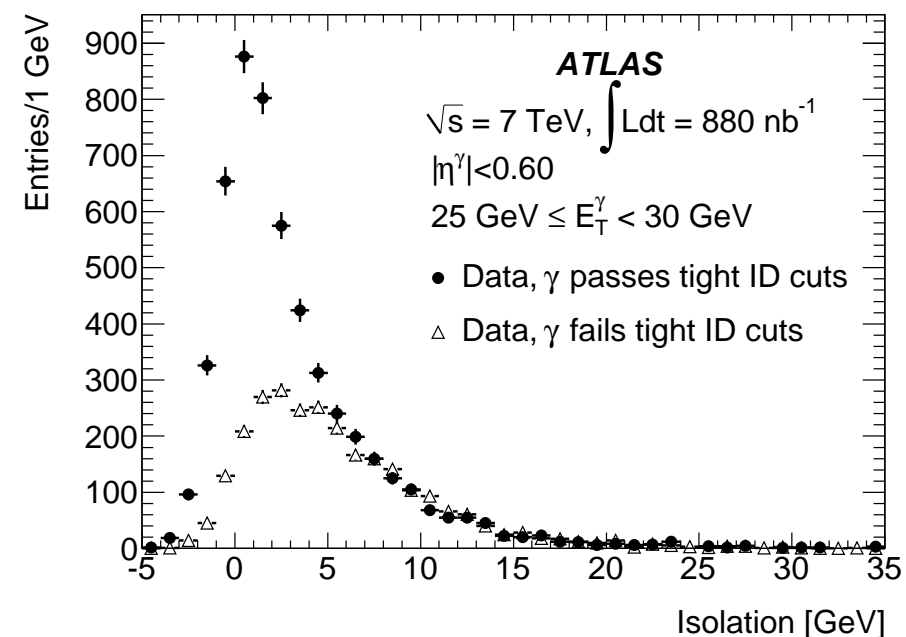
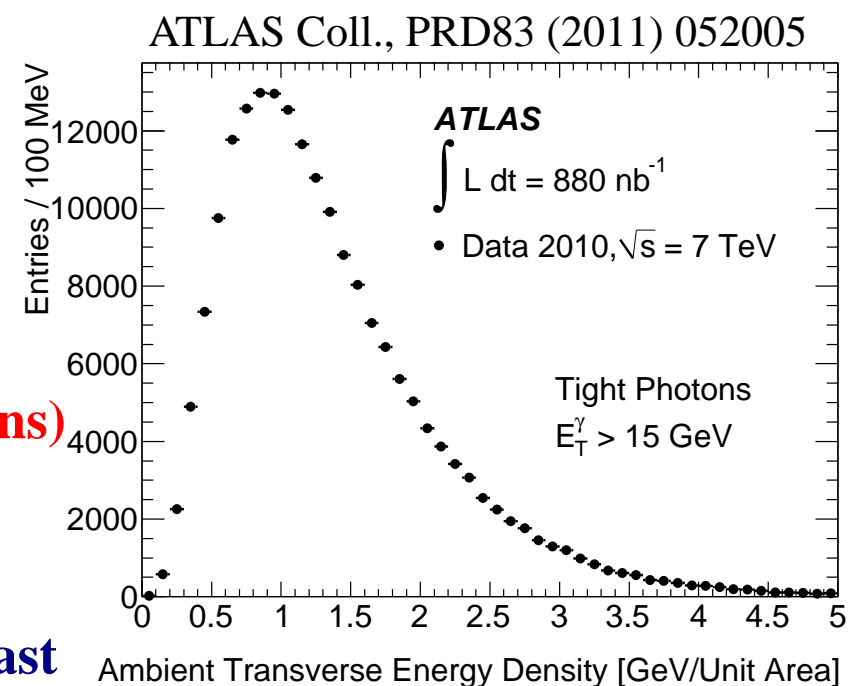
## UNCONVERTED PHOTONS



- Comparison of data-driven efficiency measurements for converted and unconverted photons performed with the 2011 and 2012 datasets as a function of the number of reconstructed primary vertex candidates ( $N_{PV}$ ), for  $|\eta^\gamma| < 0.6$ . The 2011 measurements are performed with the matrix method for photons with  $E_T^\gamma > 20$  GeV and the 2012 measurements with the electron extrapolation method for photons with  $E_T^\gamma > 30$  GeV.

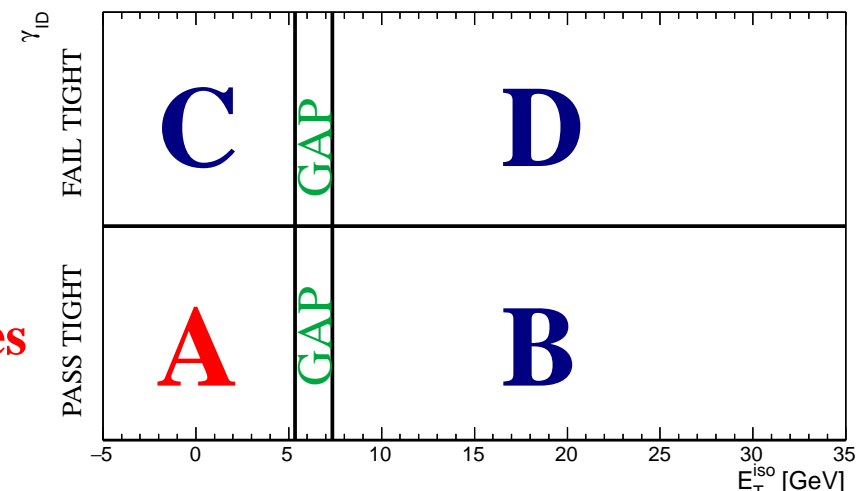
## Photon isolation in ATLAS

- $E_T^{iso}$  is corrected by subtracting the estimated contributions from the underlying event and pileup; the correction is computed on an event-by-event basis (to avoid the large fluctuations) using the jet-area method (M. Cacciari et al.)  
⇒ ambient transverse-energy density 540 MeV (in  $R = 0.4$  cone) for events with at least one photon candidate with  $E_T > 15$  GeV and exactly one PV (+170 MeV for each extra PV)
- After the correction the  $E_T^{iso}$  distribution is centered at zero with a width of 1.5 GeV in simulated signal events



## Background subtraction

- Residual background still expected even after the tight identification and isolation requirements
- A data-driven method necessary to avoid relying on detailed simulations of the background processes
- The two-dimensional sideband method:  
→ photon identification  $\gamma_{ID}$  vs  $E_T^{iso}$  plane
- It is assumed that for background events there is no correlation between  $\gamma_{ID}$  and  $E_T^{iso}$



$$\frac{N_A^{bkg}}{N_B^{bkg}} = \frac{N_C^{bkg}}{N_D^{bkg}} \quad \Rightarrow R_{bkg} \equiv \frac{N_A^{bkg} \cdot N_D^{bkg}}{N_B^{bkg} \cdot N_C^{bkg}} = 1$$

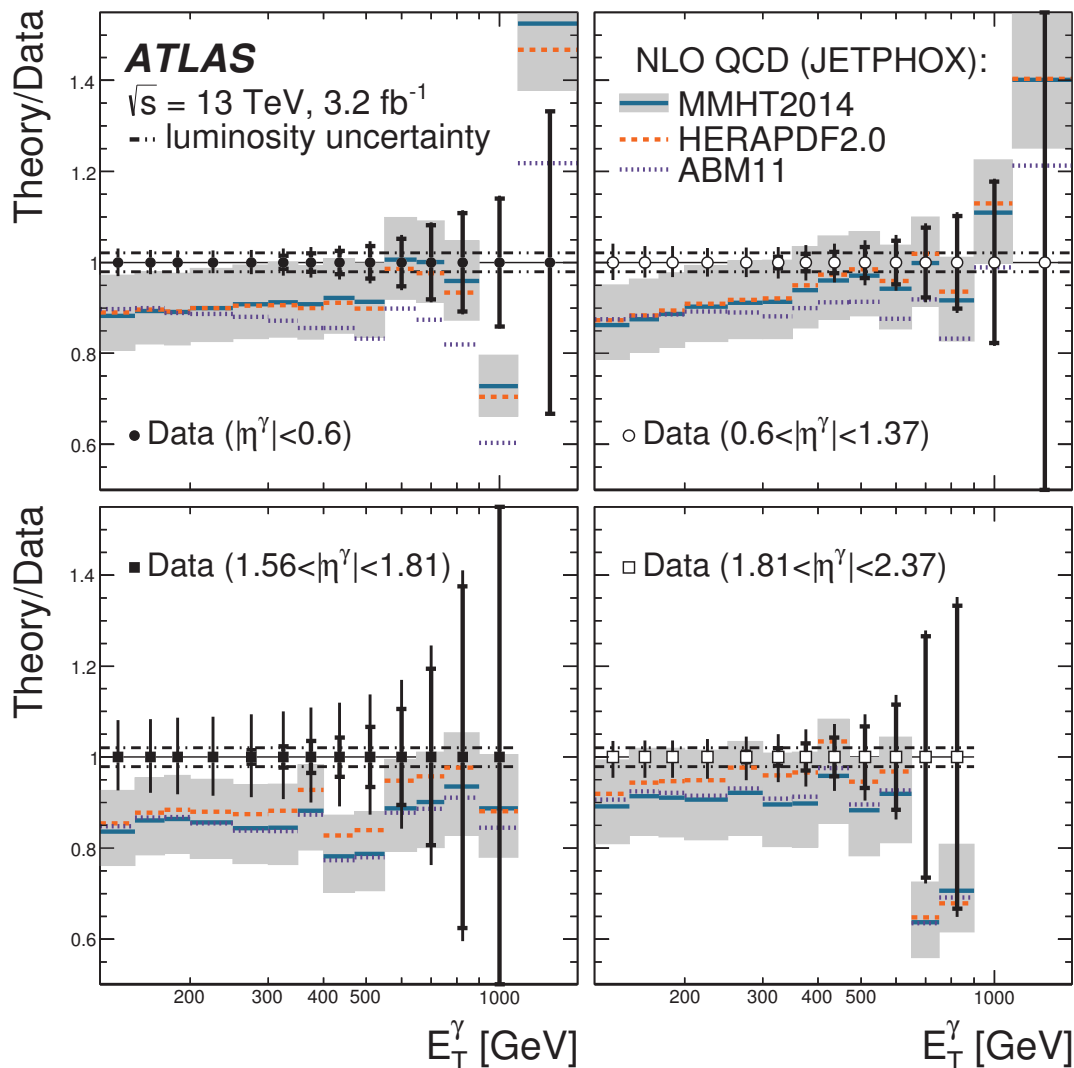
and the effects of the small signal contaminations can be accounted for by using

$$\frac{N_A - N_A^{sig}}{N_B - \epsilon_B N_A^{sig}} = \frac{N_C - \epsilon_C N_A^{sig}}{N_D - \epsilon_D N_A^{sig}}$$

to extract the signal yield  $N_A^{sig}$

the leakage fractions ( $\epsilon_K \equiv N_K^{sig}/N_A^{sig}, K = B, C, D$ ) are estimated using MC samples of signal ⇒ purity rises from 60% ( $E_T^\gamma \sim 25$  GeV) to 100% ( $E_T^\gamma \sim 300$  GeV)

## Inclusive isolated-photon cross sections vs NLO QCD



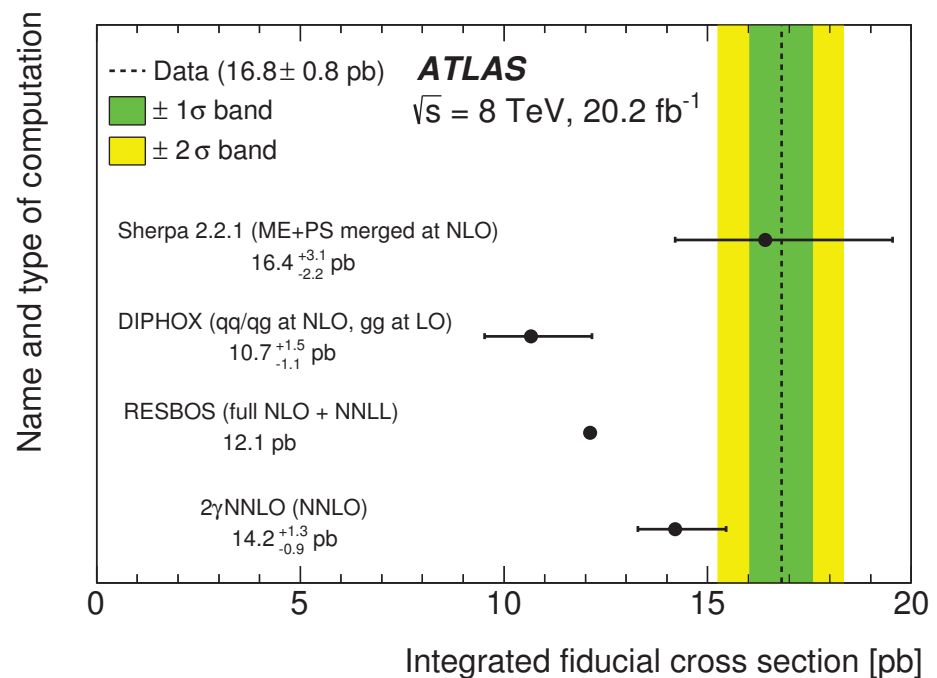
- NLO QCD predictions underestimate data by up to  $\approx 10\text{-}15\%$
- Theoretical uncertainty 10-15% much larger than experimental uncertainties
- For  $E_T^\gamma \lesssim 600 \text{ GeV}$  the measurements are systematically limited
- NLO QCD provides an adequate description of the data within uncertainties
- First measurement of inclusive photon production in the new kinematic regime opened by the LHC at  $\sqrt{s} = 13 \text{ TeV}$
- Ready for the comparison to NNLO QCD predictions (Campbell, Ellis, Williams arXiv:1612.04333)

ATLAS Coll., arXiv:1701.06882, accepted PLB

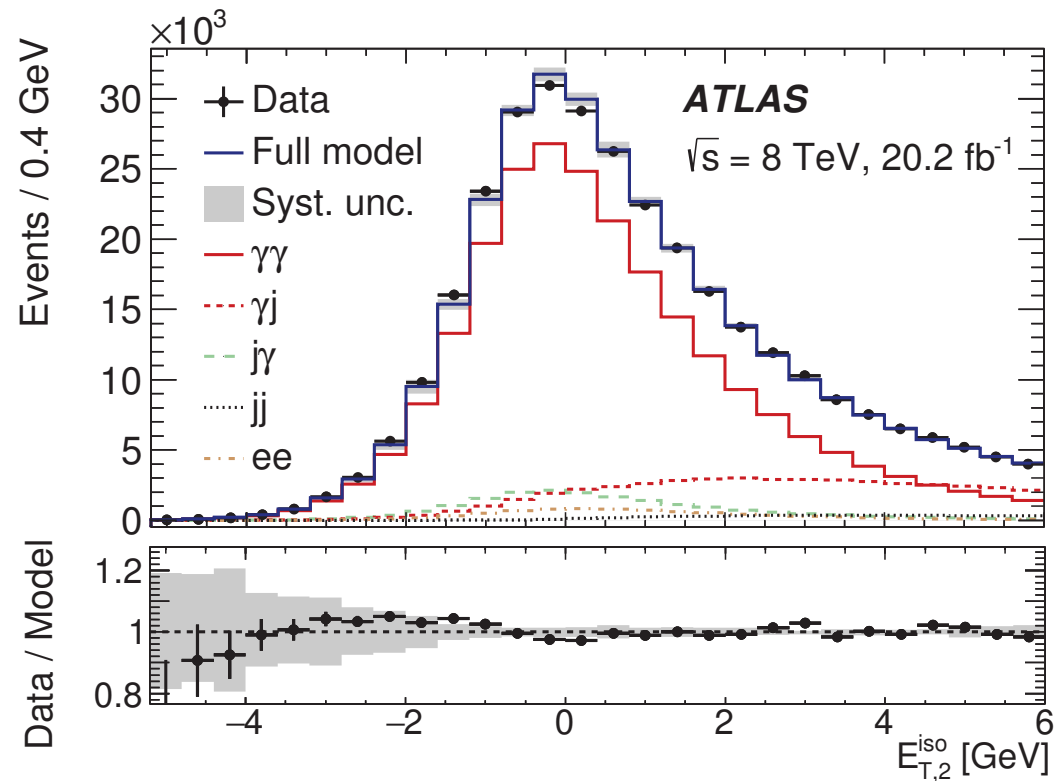
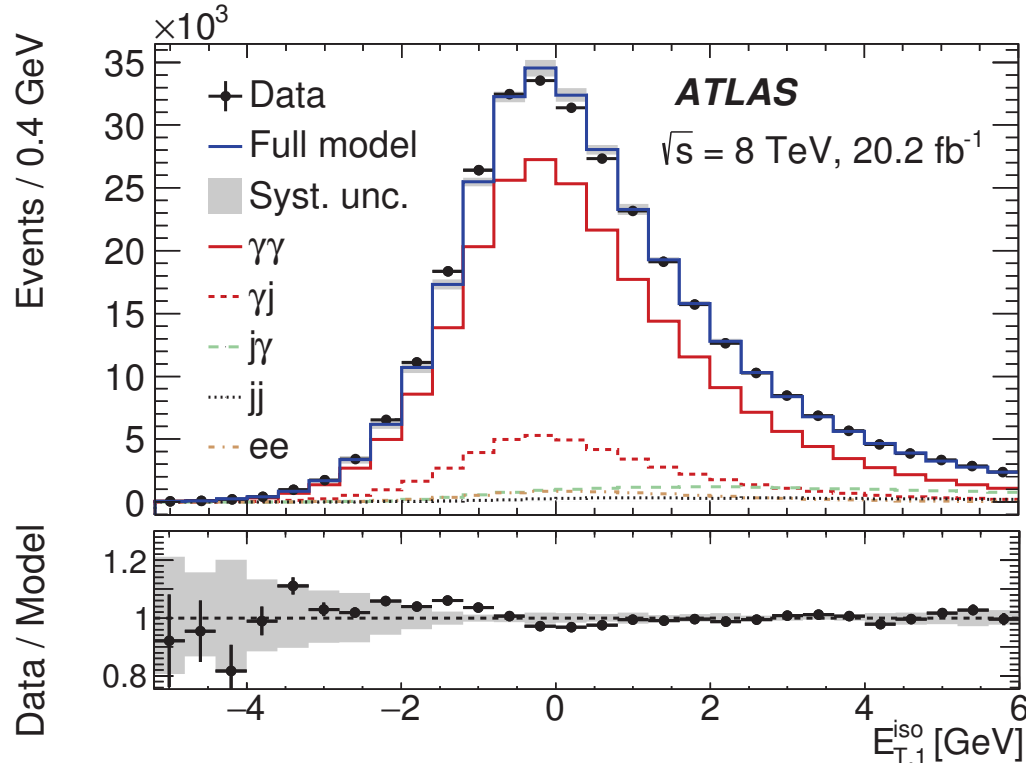
# Diphoton: sample composition and experimental uncertainties

Process	Event fraction [%]	
	Two-dimensional template fit	Matrix method
$\gamma\gamma$	$75.3 \pm 0.3$ (stat) $^{+2.6}_{-2.8}$ (syst)	$73.9 \pm 0.3$ (stat) $^{+3.1}_{-2.7}$ (syst)
$\gamma j$	$14.5 \pm 0.2$ (stat) $^{+2.7}_{-2.8}$ (syst)	$14.4 \pm 0.2$ (stat) $^{+2.0}_{-2.4}$ (syst)
$j\gamma$	$6.0 \pm 0.2$ (stat) $^{+1.4}_{-1.5}$ (syst)	$5.8 \pm 0.1$ (stat) $\pm 0.6$ (syst)
$jj$	$1.6 \pm 0.2$ (stat) $^{+0.9}_{-0.4}$ (syst)	$2.4 \pm 0.1$ (stat) $^{+0.6}_{-0.5}$ (syst)
$ee$	$2.6 \pm 0.2$ (stat) $^{+0.9}_{-0.4}$ (syst)	$3.5 \pm 0.1$ (stat) $\pm 0.4$ (syst)

Source of uncertainty	Impact on $\sigma_{\text{tot}}^{\text{fid.}}$ [%]
Photon identification efficiency	$\pm 2.5$
Modeling of calorimeter isolation	$\pm 2.0$
Luminosity	$\pm 1.9$
Control-region definition	$^{+1.5}_{-1.7}$
Track isolation efficiency	$\pm 1.5$
Choice of MC event generator	$\pm 1.1$
Other sources combined	$^{+0.8}_{-1.3}$
Total	$^{+4.5}_{-4.7}$

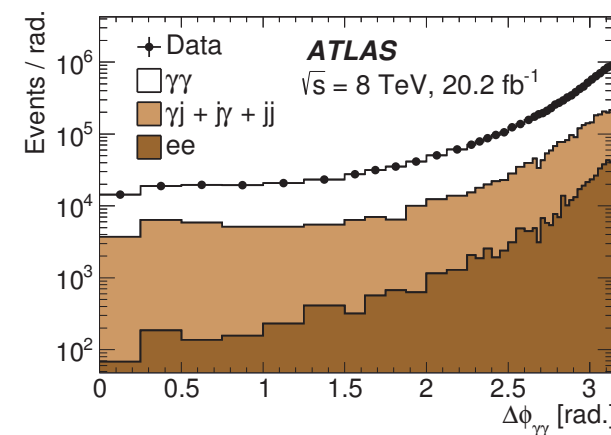
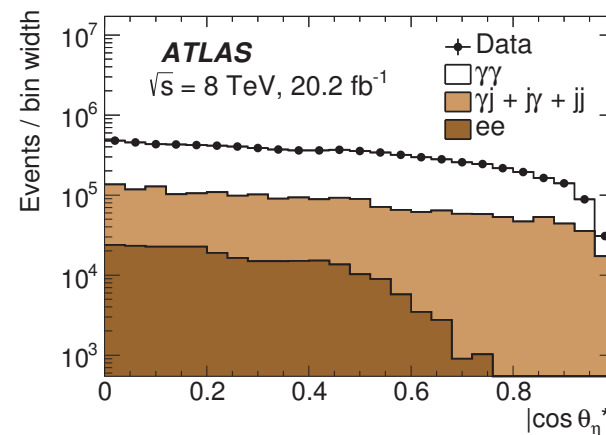
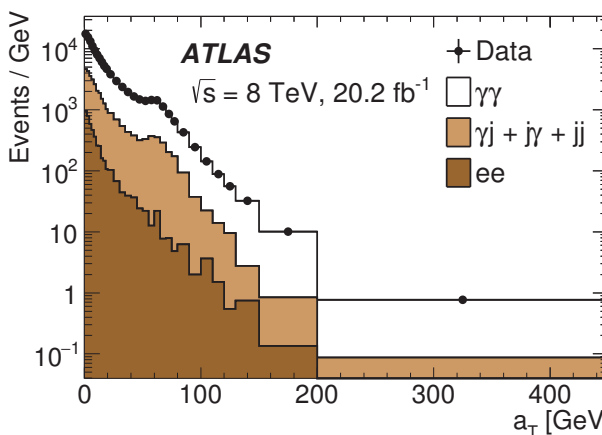
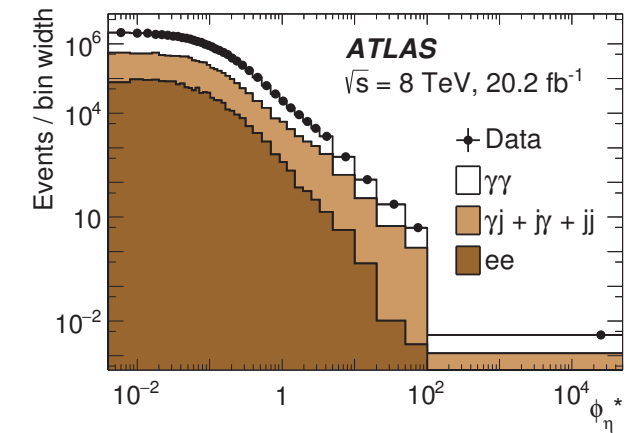
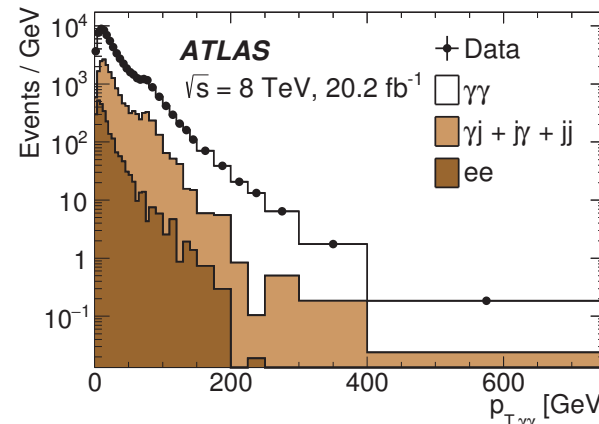
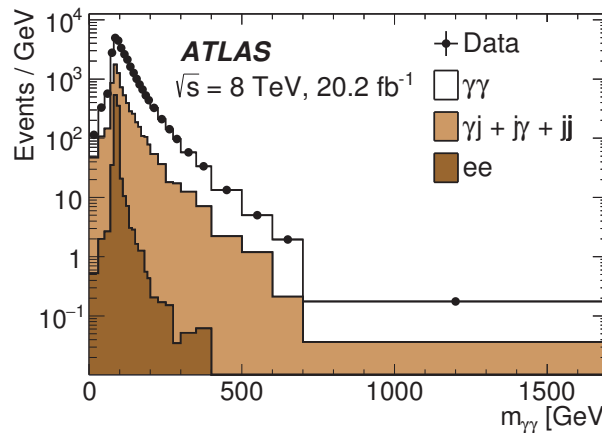


# Diphoton: $E_T^{iso}$ distributions



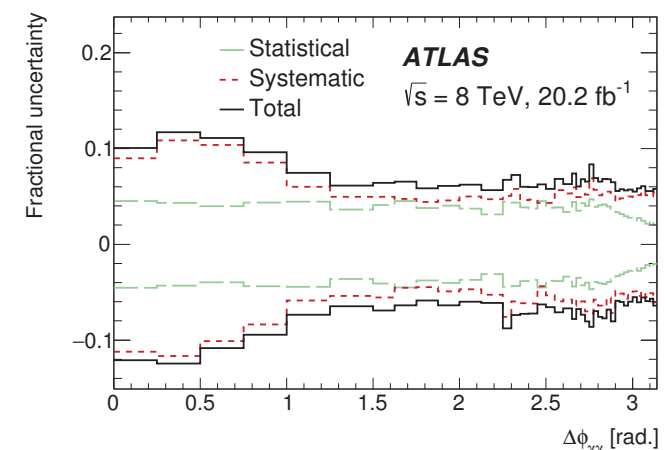
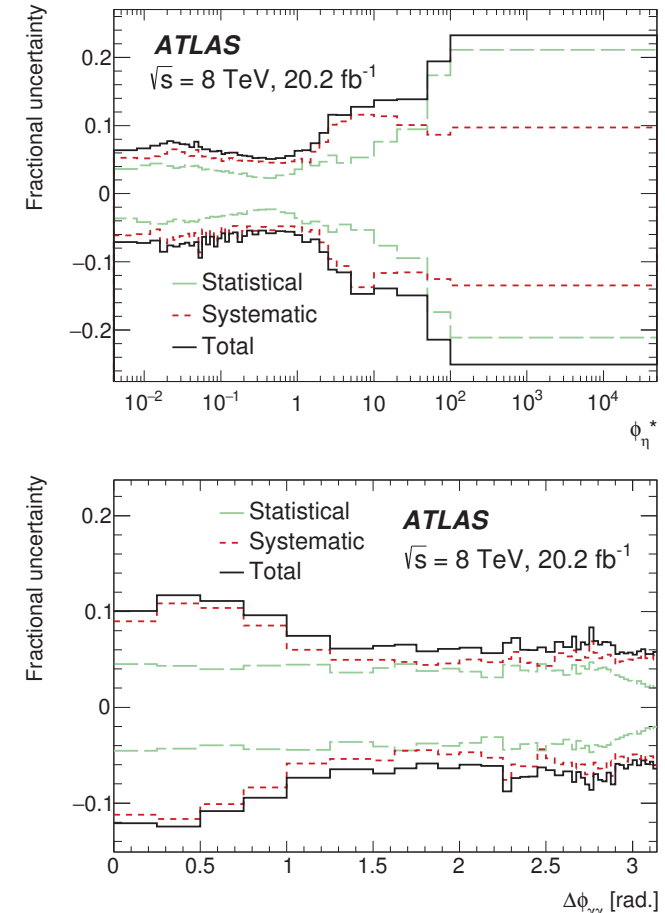
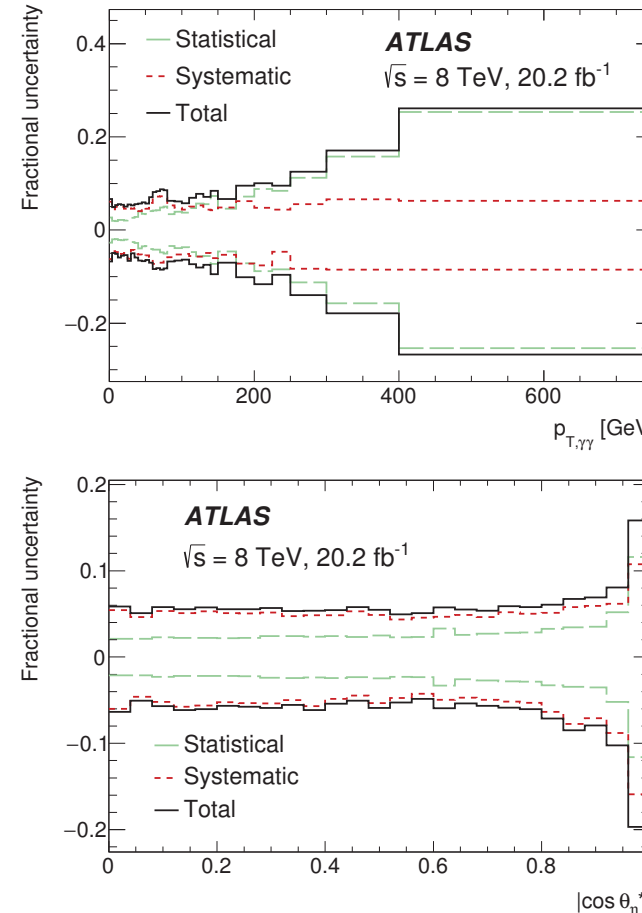
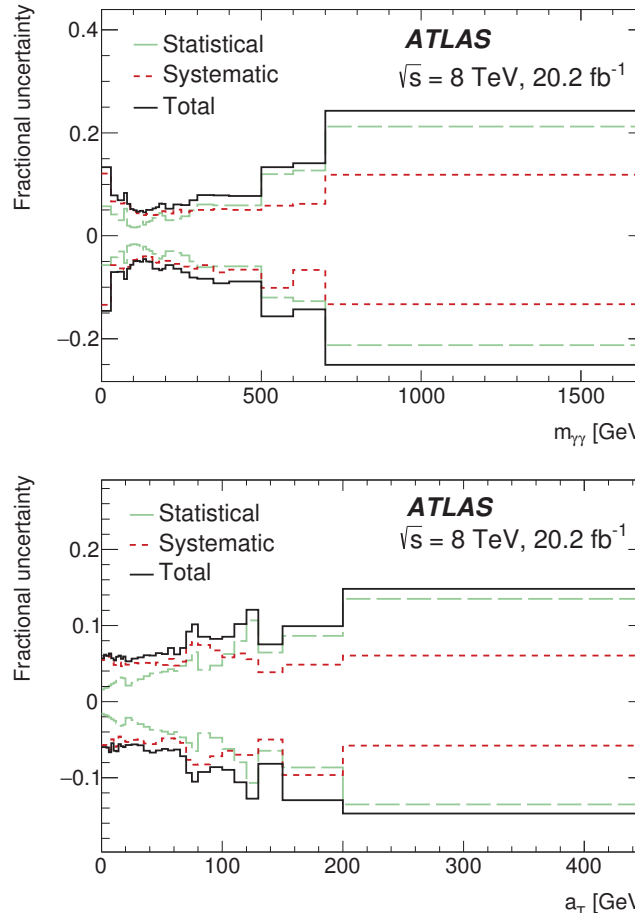
ATLAS Coll., arXiv:1704.03839

# Diphoton: sample composition



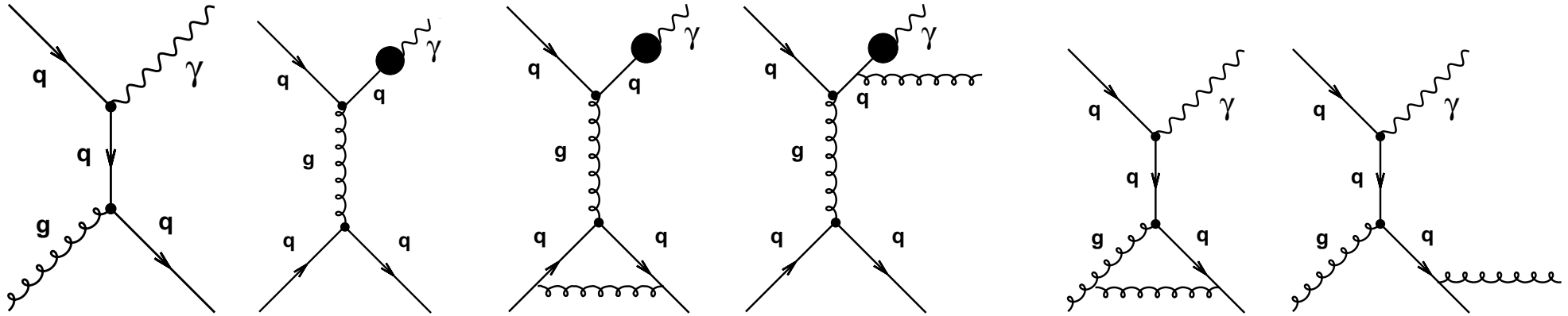
ATLAS Coll., arXiv:1704.03839

# Diphoton: experimental uncertainties



ATLAS Coll., arXiv:1704.03839

## NLO QCD calculations for inclusive photon production



$$\sigma_{pp \rightarrow \gamma + X} = \sum_{i,j,a} \int_0^1 dx_1 f_{i/p}(x_1, \mu_F^2) \int_0^1 dx_2 f_{j/p}(x_2, \mu_F^2) \hat{\sigma}_{ij \rightarrow \gamma a^+}$$

$$\sum_{i,j,a,b} \int_{z_{min}}^1 dz D_a^\gamma(z, \mu_f^2) \int_0^1 dx_1 f_{i/p}(x_1, \mu_F^2) \int_0^1 dx_2 f_{j/p}(x_2, \mu_F^2) \hat{\sigma}_{ij \rightarrow ab}$$

- The calculations includes NLO corrections for both direct-photon and fragmentation contributions; beware the components are not distinguishable beyond LO
- The calculations implement the photon isolation requirement at “parton” level:  $E_T^{iso}$  calculated with the (few) final-state partons in the perturbative QCD calculation

## NLO QCD calculations for inclusive photon production

$$\sigma_{pp \rightarrow \gamma + X} = \sum_{i,j,a} \int_0^1 dx_1 f_{i/p}(x_1, \mu_F^2) \int_0^1 dx_2 f_{j/p}(x_2, \mu_F^2) \hat{\sigma}_{ij \rightarrow \gamma a^+}$$

$$\sum_{i,j,a,b} \int_{z_{min}}^1 dz D_a^\gamma(z, \mu_f^2) \int_0^1 dx_1 f_{i/p}(x_1, \mu_F^2) \int_0^1 dx_2 f_{j/p}(x_2, \mu_F^2) \hat{\sigma}_{ij \rightarrow ab}$$

- Using the JetPhox program (**S. Catani, M. Fontannaz, J. Ph. Guillet and E. Pilon**) with

→  $\mu_R = \mu_F = \mu_f = E_T^\gamma$  (nominal)

→ proton PDF set: **CT10**

→ fragmentation function: **BFG set II**

→ Corrections for hadronisation and underlying event needed

- Theoretical uncertainties:

→ terms beyond NLO; varying  $\mu_R, \mu_F, \mu_f$  by factors 2 and 1/2 (singly or simultaneously)

→ PDF-induced uncertainties; estimated using set of PDF eigenvectors

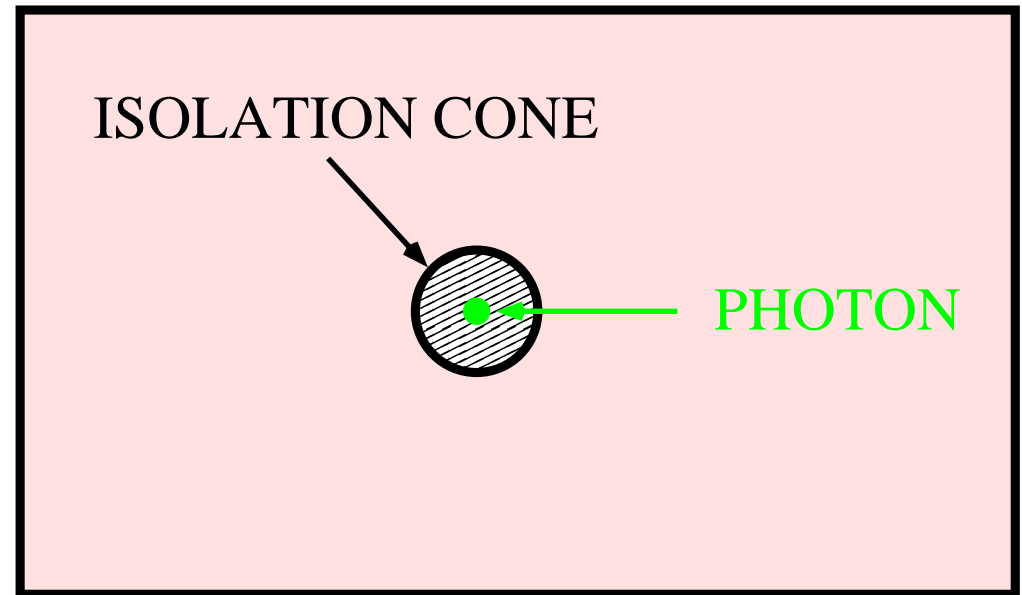
→ uncertainty on  $\alpha_s$ ; estimated using PDFs in which different values of  $\alpha_s$  are assumed

→ uncertainty on non-perturbative correction; estimated with different MCs

## Corrections for non-perturbative effects; photon isolation

- The measurements are corrected for detector effects to the “particle” level  
→ to isolated photons, where  $E_T^{iso}$  is calculated using all the final-state particles and the jet-area method is also applied

This is performed using MC simulations

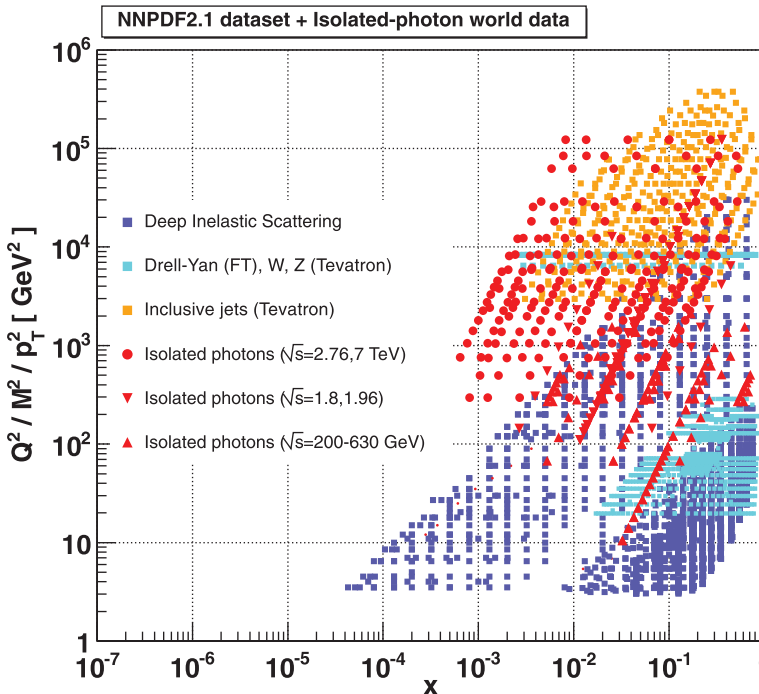


- Corrections for non-perturbative effects (hadronisation and underlying event)

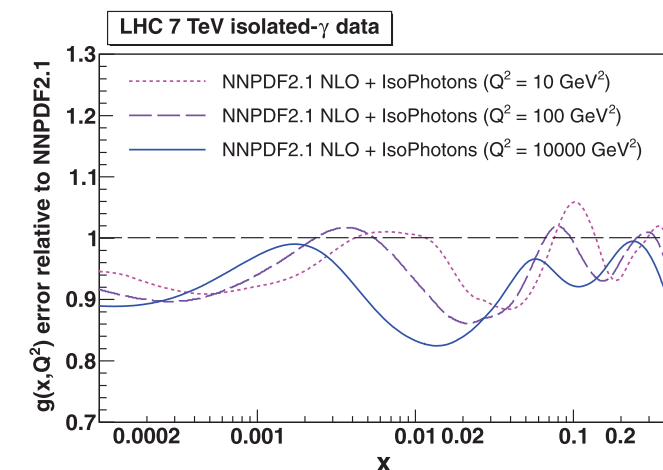
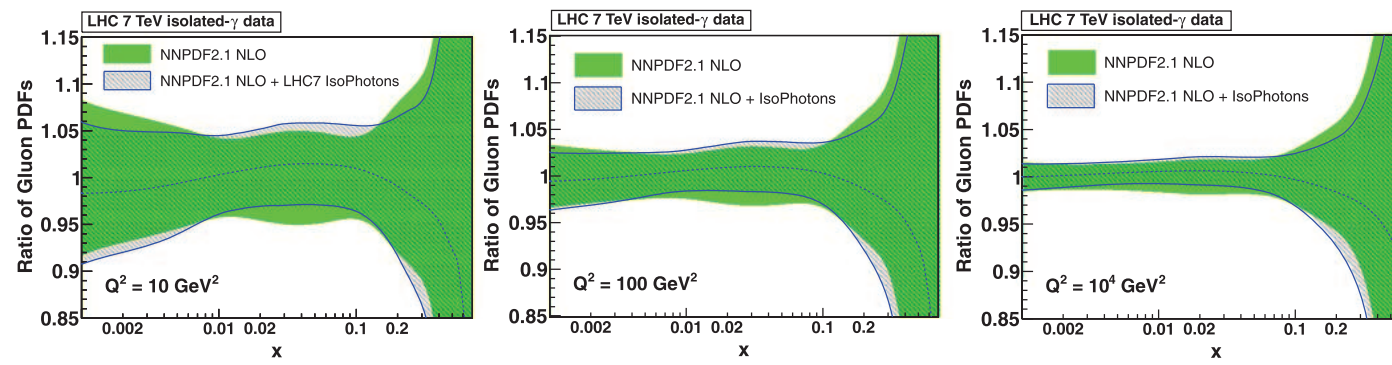
$$C_{NP} = \frac{\sigma_{\gamma+x}(\text{MC, particle-level, UE})}{\sigma_{\gamma+x}(\text{MC, parton-level, no UE})}$$

→ Less dependence on the modelling of the final state by having used the jet-area method to subtract the “extra” transverse energy contribution to  $E_T^{iso}$

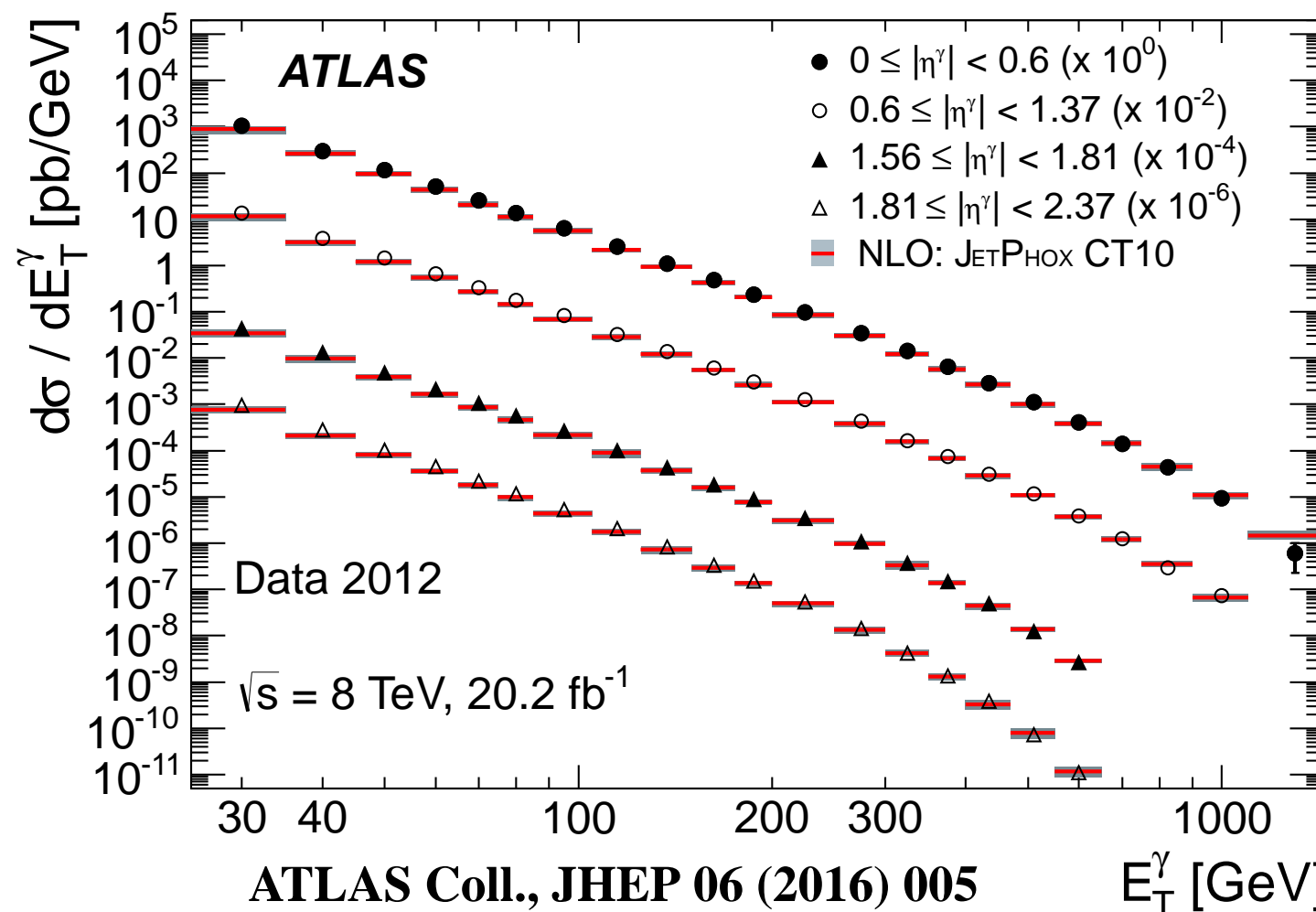
# Impact of inclusive isolated photon measurements at LHC on PDFs



- Analysis by D. d'Enterria and J. Rojo (NPB860,2012,311)
- Study of the impact on the gluon density of existing isolated-photon measurements from a variety of experiments, from  $\sqrt{s} = 200$  GeV up to 7 TeV
  - those at LHC are the more constraining datasets
  - reduction of gluon uncertainty up to 20%
  - localised in the range  $x \approx 0.002$  to 0.05
- ⇒ improved predictions for low mass Higgs production in gluon fusion, PDF-induced uncertainty decreased by 20%



## Inclusive isolated-photon production in $pp$ collisions at $\sqrt{s} = 8$ TeV

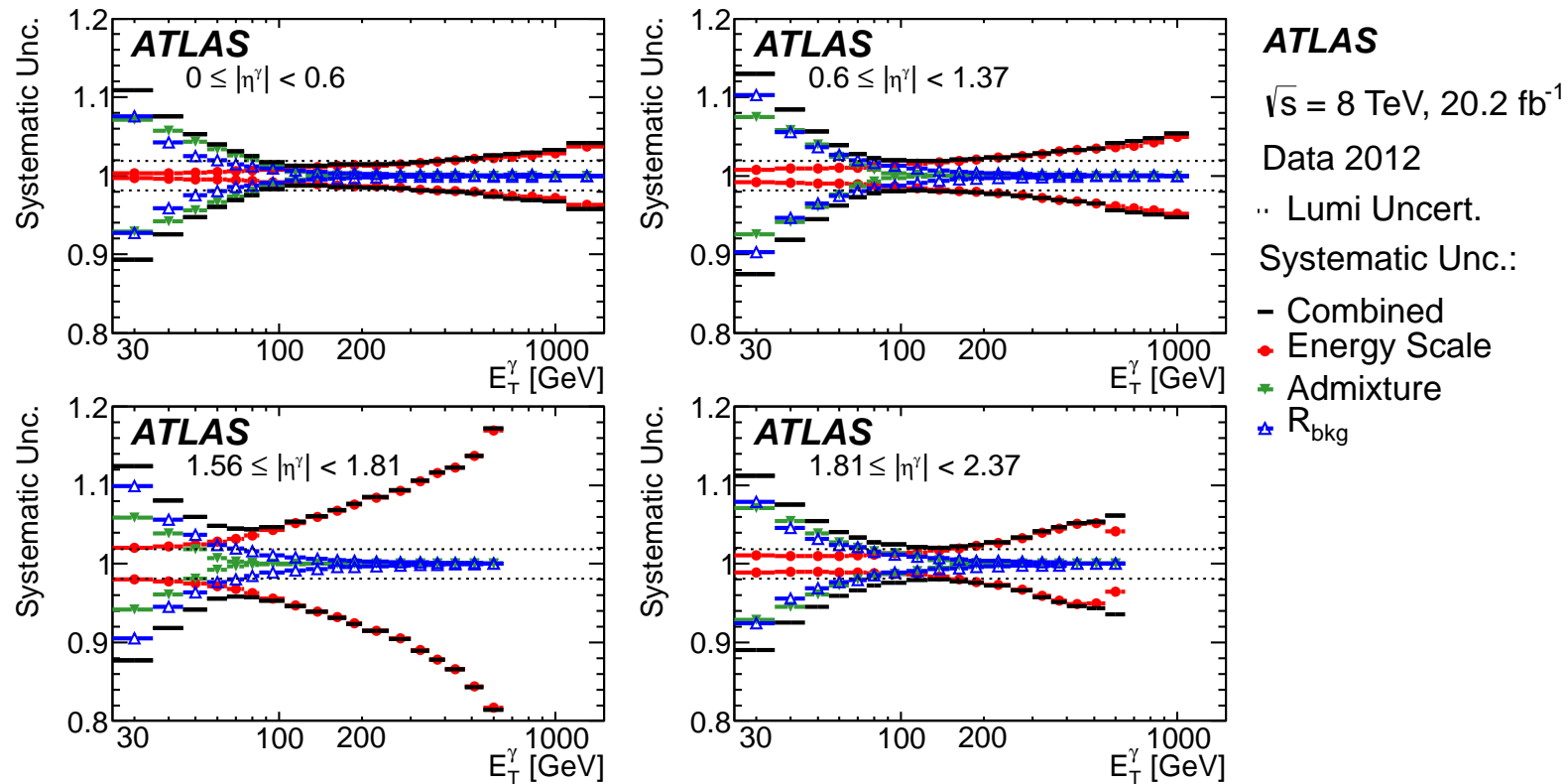


- Measurement of  $d\sigma/dE_T^\gamma$  for  $25 < E_T^\gamma < 1500$  GeV and different ranges in  $\eta^\gamma$  using  $\mathcal{L} = 20.2 \text{ fb}^{-1}$  of  $pp$  collision data at  $\sqrt{s} = 8$  TeV
- $E_T^{\text{iso}} < 4.2 \cdot 10^{-3} \cdot E_T^\gamma + 4.8 \text{ GeV}$
- The measurement covers ten orders of magnitude in cross section
- First measurement of photon production with  $E_T^\gamma > 1$  TeV

- Significant improvement in experimental uncertainties over the previous measurements
- Good description (in log scale) of the data by NLO QCD calculations using JetPhox

# Major experimental uncertainties

ATLAS Coll., JHEP 06 (2016) 005



- The uncertainty on the photon energy scale\* (about 1% except in the region  $1.56 < |\eta^\gamma| < 1.81$ ) is dominant at high  $E_T^\gamma$
- The uncertainty on the correlation in the background ( $\pm 10\%$ ) dominates at low  $E_T^\gamma$ , but negligible at high  $E_T^\gamma$
- The uncertainty on the admixture of direct and fragmentation photons increases at low  $E_T^\gamma$

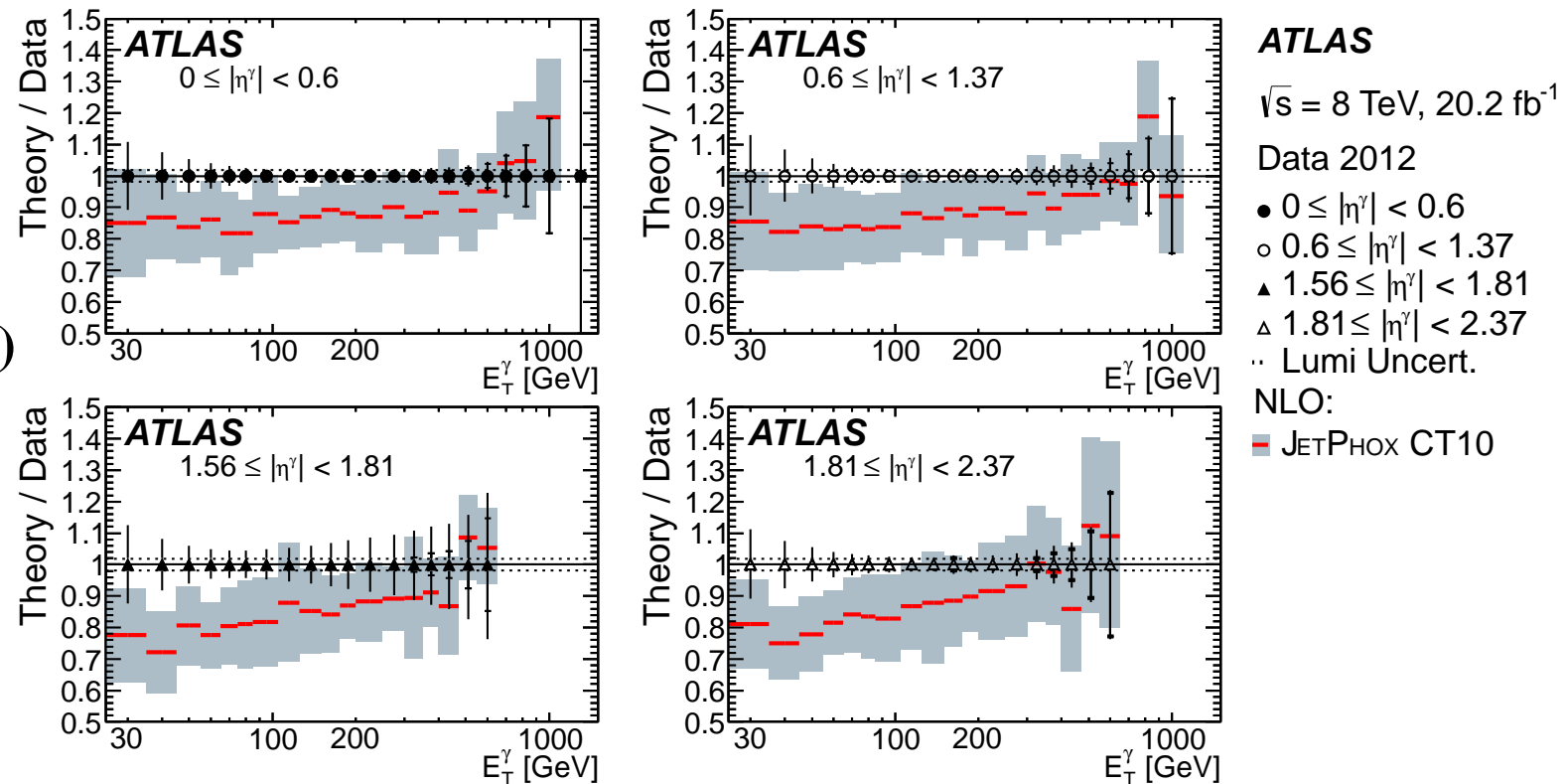
\* (ATLAS Collaboration, Eur. Phys. J. C74 (2014) 3071)

# Inclusive isolated-photon cross sections vs NLO QCD

ATLAS Coll., JHEP 06 (2016) 005

Theoretical  
uncertainties  
much larger than(!)

experimental  
uncertainties



- Comparison to NLO QCD calculation using the JetPhox program
  - a similar trend is observed at low  $E_T^\gamma$  in all  $|\eta^\gamma|$  regions, the NLO QCD predictions underestimate the data by  $\approx 20\%$
  - the theoretical uncertainty (12-20%) prevents a more precise test of the SM predictions
- Halving the measured uncertainties compared to previous measurements
  - ⇒ useful constraint on proton PDFs once included in a global fit